JEM Journal of Experimental Medicine

ARTICLE

Broad and potent neutralizing human antibodies to tick-borne flaviviruses protect mice from disease

Marianna Agudelo[1], Martin Palus[2,3]*, Jennifer R. Keeffe[4]*, Filippo Bianchini[1,5], Pavel Svoboda[3,6], Jiří Salát[2,3], Avery Peace[7], Anna Gazumyan[1], Melissa Cipolla[1], Tania Kapoor[1], Francesca Guidetti[1], Kai-Hui Yao[1], Jana Elsterová[2,3], Dana Teislerová[8], Aleš Chrdle[8,9,10], Václav Hönig[2,3], Thiago Oliveira[1], Anthony P. West Jr.[4], Yu E. Lee[4], Charles M. Rice[7], Margaret R. MacDonald[7], Pamela J. Bjorkman[4], Daniel Růžek[2,3], Davide F. Robbiani[1,5], and Michel C. Nussenzweig[1,11]

Tick-borne encephalitis virus (TBEV) is an emerging human pathogen that causes potentially fatal disease with no specific treatment. Mouse monoclonal antibodies are protective against TBEV, but little is known about the human antibody response to infection. Here, we report on the human neutralizing antibody response to TBEV in a cohort of infected and vaccinated individuals. Expanded clones of memory B cells expressed closely related anti-envelope domain III (EDIII) antibodies in both groups of volunteers. However, the most potent neutralizing antibodies, with IC_{50}s below 1 ng/ml, were found only in individuals who recovered from natural infection. These antibodies also neutralized other tick-borne flaviviruses, including Langat, louping ill, Omsk hemorrhagic fever, Kyasanur forest disease, and Powassan viruses. Structural analysis revealed a conserved epitope near the lateral ridge of EDIII adjoining the EDI–EDIII hinge region. Prophylactic or early therapeutic antibody administration was effective at low doses in mice that were lethally infected with TBEV.

Introduction

Tick-borne flaviviruses are responsible for a series of emerging infectious diseases including fatal encephalitis. Like other flaviviruses, the tick-borne encephalitis virus (TBEV) envelope protein (E) is composed of three structural domains (envelope domains I–III [EDI–EDIII]; Füzik et al., 2018; Pulkkinen et al., 2018). Mouse monoclonal antibodies against EDIII, an Ig-like domain that mediates host cell attachment, are potent neutralizers of TBEV (Baykov et al., 2014; Füzik et al., 2018; Levanov et al., 2010; Matveev et al., 2020; Phillpotts et al., 1985; Rey et al., 1995; Yang et al., 2019).

TBEV is one of the six flaviviruses transmitted by ticks causing human disease (Gould and Solomon, 2008; Kuno et al., 1998; LaSala and Holbrook, 2010). These include Omsk hemorrhagic fever virus (OHFV) in Russia; Kyasanur forest disease virus (KFDV) in India; Alkhurma virus in Saudi Arabia; louping ill virus (LIV) in the United Kingdom, Ireland, Norway, Denmark, and Russia; and Powassan virus in the United States and Canada. Upwards of 10,000 TBEV cases per year are reported, with a trend for increased incidence in recent years and emergence of the disease in new geographic regions (Beauté et al., 2018; Girl et al., 2020; Kollaritsch et al., 2011; Morens and Fauci, 2020; Smura et al., 2019; Süss et al., 2006; Yoshii, 2019; Zeman and Bene, 2004).

The bite of an infected tick, or the consumption of unpasteurized milk from infected animals, causes a biphasic illness, which begins with a period of influenza-like symptoms followed by the development of neurological disease (tick-borne encephalitis [TBE]). There is no specific therapy for TBE, and treatment is limited to supportive care. For those individuals who survive, long-term sequelae are common (Bogovič et al., 2018b; Caini et al., 2012; Cisak et al., 2010; Donoso-Mantke et al., 2011; Holzmann, 2003; Holzmann et al., 2009; Kaiser, 2008).

Although TBEV vaccines are available, immunity requires regular boosting, and vaccination is less effective in the young and elderly. Vaccination requires administration of three separate doses spaced over up to 2 yr, with booster doses recommended at intervals of 3–5 yr (World Health Organization,

[1]Laboratory of Molecular Immunology, The Rockefeller University, New York, NY; [2]Institute of Parasitology, Biology Centre of the Czech Academy of Sciences, České Budějovice, Czech Republic; [3]Veterinary Research Institute, Brno, Czech Republic; [4]Division of Biology and Biological Engineering, California Institute of Technology, Pasadena, CA; [5]Institute for Research in Biomedicine, Università della Svizzera italiana, Bellinzona, Switzerland; [6]Department of Pharmacology and Pharmacy, Faculty of Veterinary Medicine, University of Veterinary and Pharmaceutical Sciences Brno, Brno, Czech Republic; [7]Laboratory of Virology and Infectious Disease, The Rockefeller University, New York, NY; [8]Hospital České Budějovice, České Budějovice, Czech Republic; [9]Faculty of Social and Health Sciences, University of South Bohemia, České Budějovice, Czech Republic; [10]Royal Liverpool University Hospital, Liverpool, UK; [11]Howard Hughes Medical Institute, The Rockefeller University, New York, NY.

*M. Palus and J.R. Keeffe contributed equally to this paper; Correspondence to Michel C. Nussenzweig: nussen@rockefeller.edu; Davide F. Robbiani: drobbiani@irb.usi.ch; Daniel Růžek: ruzekd@paru.cas.cz; Pamela J. Bjorkman: bjorkman@caltech.edu.

© 2021 Agudelo et al. This article is available under a Creative Commons License (Attribution 4.0 International, as described at https://creativecommons.org/licenses/by/4.0/).

Downloaded from http://rupress.org/jem/article-pdf/218/5/e20210236/1803798/jem_20210236.pdf by guest on 18 January 2024

2019). Breakthrough TBEV infection occurs despite vaccination (Dobler et al., 2020; Lotrič-Furlan et al., 2017).

Recovered individuals can produce potent serologic neutralizing activity against TBEV, and the serum can be cross-reactive against other tick-borne flaviviruses, but the nature of the antibodies that mediate these effects is not known (Calisher et al., 1989; Mansfield et al., 2011). Postexposure prophylaxis with hyperimmune plasma Ig from vaccinated donors provides protection if administered within 3 d of an infected tick bite (Kreil et al., 1998; Pen'evskaia and Rudakov, 2010). However, this practice was discontinued outside of Russia due to anecdotal evidence of adverse events in children and the concern of possible antibody-dependent enhancement of disease (Halstead, 2014; Phillpotts et al., 1985; Ruzek et al., 2019).

Here, we report on the molecular properties of human anti-TBEV antibodies with exceptional neutralizing potency and breadth that are effective in protection and early therapy in mice.

Results

Serological responses in a TBEV-infected cohort

We analyzed sera from 141 individuals hospitalized with TBE during the 2011 and 2018 outbreaks in the Czech Republic (see Materials and methods). Samples were obtained at the time of hospitalization during the encephalitic phase of disease (Fig. 1 A; Holzmann, 2003). In agreement with previous reports (Bogovič et al., 2018a; Bogovic and Strle, 2015), the cohort was characterized by higher incidence in males (61.1%) and older individuals (mean age, 49 yr; Table S1). Control sera were also obtained from 168 randomly selected blood bank donors and 10 individuals vaccinated against TBEV (Table S1). All sera were screened by ELISA at a dilution of 1:500 for the presence of IgG antibodies binding to the EDIII of TBEV (Fig. 1 B). The signal in infected individuals was significantly higher than in the vaccinated and blood donor groups ($P = 0.0005$ and $P < 0.0001$ by ANOVA using Tukey's correction, respectively; Fig. 1 B). There was no correlation between TBEV EDIII ELISA reactivity and age, duration of hospitalization, severity of infection, or gender of patient, but serum EDIII binding did correlate positively with patient IgM ($P = 0.0029$) and IgG ($P < 0.0001$) levels at the time of hospitalization (Fig. S1, A–F).

To evaluate serum neutralizing activity, samples obtained from recovered and vaccinated individuals were screened at a 1:6×10^5 dilution for neutralization using luciferase-expressing TBEV reporter virus particles (RVPs; see Materials and methods; Pierson et al., 2006). Neutralizing activity ranged from complete to undetectable and was significantly lower in vaccinees ($P < 0.0001$; Fig. 1 C). Neutralization correlated positively with patient IgM levels at the time of hospitalization ($P < 0.0001$) and EDIII binding in ELISA ($P = 0.0004$); otherwise, there was no correlation with demographic or clinical data (Fig. S1, G–M). The half-maximal neutralizing titers (NT_{50}) for the top 28 infected individuals varied from 0.37 to 6.7×10^6 (Fig. 1, D and E). In contrast, vaccinees showed NT_{50}s of $0.32–1.0 \times 10^4$ (Fig. S1, N and O). We conclude that individuals hospitalized for TBEV infection show a broad distribution of EDIII binding and neutralizing activity that is generally higher than the vaccinees in this cohort.

B cell memory convergence on specific antibody genes

To characterize the anti-TBEV antibodies, we purified B cells that bind to TBEV EDIII from peripheral blood of six infected individuals (orange in Fig. 1, D and E) and three vaccinees (see Materials and methods; Fig. 2, A–D; and Fig. S2 A). The frequency of TBEV EDIII–specific B cells was higher in the infected group (0.067–0.31%) compared with vaccinees (1.28×10^{-3}–5.95×10^{-3}%). In total, 776 IgG antibody heavy and light chain gene pairs were amplified by RT-PCR and sequenced (see Materials and methods; Fig. 2, B and D; and Table S2). The average somatic hypermutation in Ig heavy and light chain genes (Ig variable heavy gene [IGVH], Ig variable kappa gene [IVGK], and Ig variable light gene [IGVL]) was 18 and 9 nt, respectively, complementarity-determining region 3 (CDR3) length was normal (mean CDRH3 length of 13.5 and mean CDRL3 length of 9.4), and hydrophobicity was slightly increased compared with control ($P < 0.0001$; Fig. S2, B–D; Briney et al., 2019; Rock et al., 1994). As with other viral pathogens, including HIV-1, Zika, hepatitis B, and SARS-CoV-2 (Robbiani et al., 2017; Robbiani et al., 2020; Scheid et al., 2011; Wang et al., 2020; West et al., 2012), many of the sequences were found in expanded B cell clones (37.9%; Fig. 2, B and D).

Sequence analysis revealed antibodies with similar features within and between individuals (Fig. 2, B, D, and E; Table S2; and Table S3). For example, VH1–69 and VH3–48 accounted for 59.2% and 7.5% of all clonal sequences, respectively (shades of blue and red in Fig. 2, B and D). In addition, related sequences containing these VH genes were found in multiple donors (purple lines in Fig. 2 E). Usage of VH1–69, VH3–30, VK2–28, VK1–33, and VL4–69 genes in infected donors was significantly overrepresented ($P < 0.01$); VH3–48, VK1–5, and VL2–14 genes were also enriched, although not significantly (Fig. S3, A–C). In some cases, including clonally expanded IGVH1–69/Ig variable kappa gene 2–28 (IGVK2–28) and IGVH3–48/IGVK1–5 antibodies, sequence similarities between individual donors extended to the IGH and IGL CDR3s (Fig. S2, D and E; and Table S3). We conclude that the memory B cell response to the TBEV EDIII converges toward specific antibody genes.

Potent and broadly cross-reactive anti-TBEV antibodies

59 antibodies (46 from convalescent and 13 from vaccinated donors; Table S4) were cloned, recombinantly expressed, and tested in ELISA for binding to EDIII proteins corresponding to all three TBEV subtypes: Western European ($TBEV^{WE}$), Far Eastern ($TBEV^{FE}$), and Siberian ($TBEV^{Si}$; Fig. 3 A, Fig. S4 A, and Table S5). All but 1 of the 59 antibodies bound to all three EDIIIs with similar half-maximal effective concentrations (EC_{50}) ranging from 0.2 to 12 ng/ml (Fig. 3 B and Table S5).

When tested for neutralizing activity, 43 out of 46 antibodies obtained from infected donors neutralized TBEV RVPs with half-maximal inhibitory concentrations (IC_{50}s) as low as 0.02 ng/ml (Fig. 3, C and D; and Table S5). In contrast, the best antibody obtained from vaccinated donors was over two orders of magnitude less potent (IC_{50} of 8.3 ng/ml). Seven antibodies, all

Downloaded from http://rupress.org/jem/article-pdf/218/5/e20210236/1803798/jem_20210236.pdf by guest on 18 January 2024

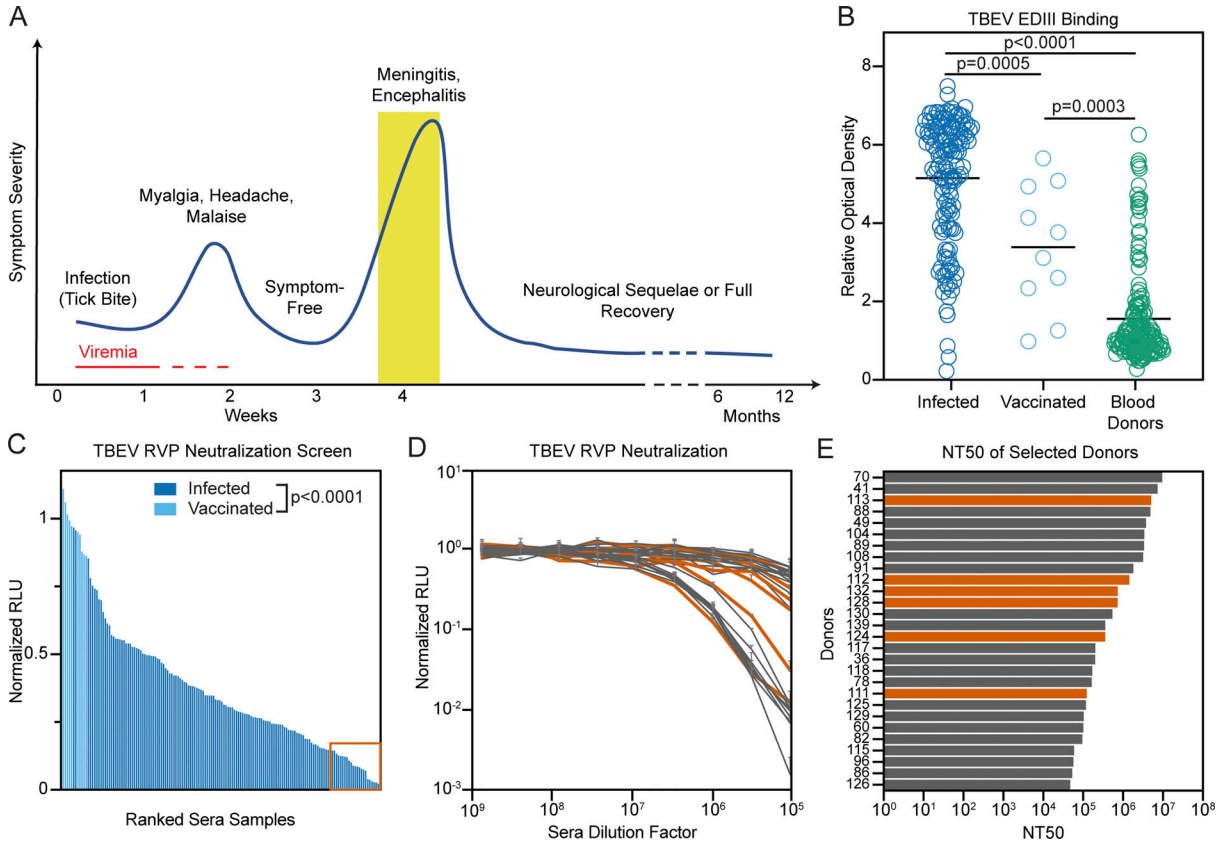

Figure 1. **Screening individuals for TBEV antibodies. (A)** Diagrammatic representation of the clinical course of TBE. The approximate time of serum collection is shown in yellow. **(B)** TBEV EDIII IgG ELISA. Graph shows optical density measurement (y axis) relative to a negative control serum for samples from 141 TBEV-infected individuals, 10 TBEV vaccinees, and 168 random blood donors (1:500 dilution) measured in singlicate. P = 0.0005 for infected versus vaccinees; P < 0.0001 for infected versus blood donors; P = 0.0003 for vaccinees versus blood donors; calculated by one-way ANOVA followed by Tukey's test. Horizontal lines indicate the mean. **(C)** TBEV RVP neutralization screening. Graph shows ranked serum neutralizing activity (1:600,000 dilution) against TBEV RVPs (average of duplicate wells) relative to no serum control. The orange box (bottom right) indicates the 28 best neutralizers of 141 TBEV-infected individuals and 10 TBEV vaccinees tested. P < 0.0001; calculated using two-tailed Mann–Whitney test. **(D)** TBEV RVP neutralization curves. Plot shows representative neutralization curves for each of the 28 most potent sera from C. Representative of two experiments, each performed in triplicate. Error bars indicate standard deviation. **(E)** Ranked NT_{50}s for the top 28 individuals. Average of two independent experiments. In D and E, orange indicates the donors of PBMCs for antibody cloning. Related to Fig. S1 and Table S1. RLU, relative light units.

isolated from infected donors, were potent neutralizers of TBEV RVPs with IC_{50}s below 1 ng/ml (Fig. 3 D). Four of these antibodies were also evaluated for neutralization of authentic TBEV (Fig. 3, E and F). All four antibodies showed potent activity, with IC_{50}s ranging from 35.9 to 268.8 ng/ml (Table S5).

To determine whether the TBEV antibodies cross-react with related viruses, we screened them at a single concentration (1 µg/ml) for binding to the EDIIIs of Langat virus (LGTV), LIV, OHFV, KFDV, and Powassan lineage I and II viruses (Powassan-LB virus [POWV-LB] and Powassan deer tick virus [POWV-DTV]; see Materials and methods and Fig. S4, B and C). Broad cross-reactivity was observed for many of the antibodies tested (Fig. S4, B and C). To determine whether the antibodies are also broadly neutralizing, we screened them against RVPs corresponding to the same panel of tick-borne viruses. When tested at a concentration of 1 µg/ml, most of the IGHV1–69 antibodies neutralized LGTV, LIV, POWV-LB, and POWV-DTV, and one of the IGVH3–48/IGVK1–5 antibodies neutralized all RVPs except POWV-LB (Fig. S4, B and C). IC_{50}s against the flavivirus RVP panel were <10 ng/ml for several of the cross-reactive antibodies (Fig. 3 G; Fig. S4, D–I; and Table S5). For example, an IGVH3–48/IGVK1–5 antibody, T056, is a potent neutralizer of LGTV, LIV, and OHFV, with IC_{50} values ≤1 ng/ml. We conclude that some TBEV neutralizing antibodies are broadly active against tick-borne flaviviruses.

Antibody T025 binds to the EDIII lateral ridge

To gain insights into the mechanism of neutralization by human anti-TBEV antibodies, we solved crystal structures of the antigen-binding fragment (Fab) from the broad and potent antibody T025 (IGVH3–30/IGVK3–15) in complex with the EDIII domains of all three subtypes of TBEV (Fig. 4, Fig. S5, and Table S6). The structure of the T025 Fab–$TBEV^{WE}$ EDIII complex revealed that the antibody binds the lateral ridge of EDIII in the proximity of the EDI–EDIII hinge region, making both heavy chain (HC) and light chain (LC) contacts to the EDI–EDIII hinge and the BC loop and light chain contacts to the DE loop of the EDIII (Fig. 4 A). The antibody contacts EDIII using CDRH2, CDRH3, CDRL1, and CDRL3, and buries 598 $Å^2$ of surface area on the EDIII (333 $Å^2$ by the V_H and 265 $Å^2$ by the V_L). T025 inserts

Downloaded from http://rupress.org/jem/article-pdf/218/5/e20210236/1803798/jem_20210236.pdf by guest on 18 January 2024

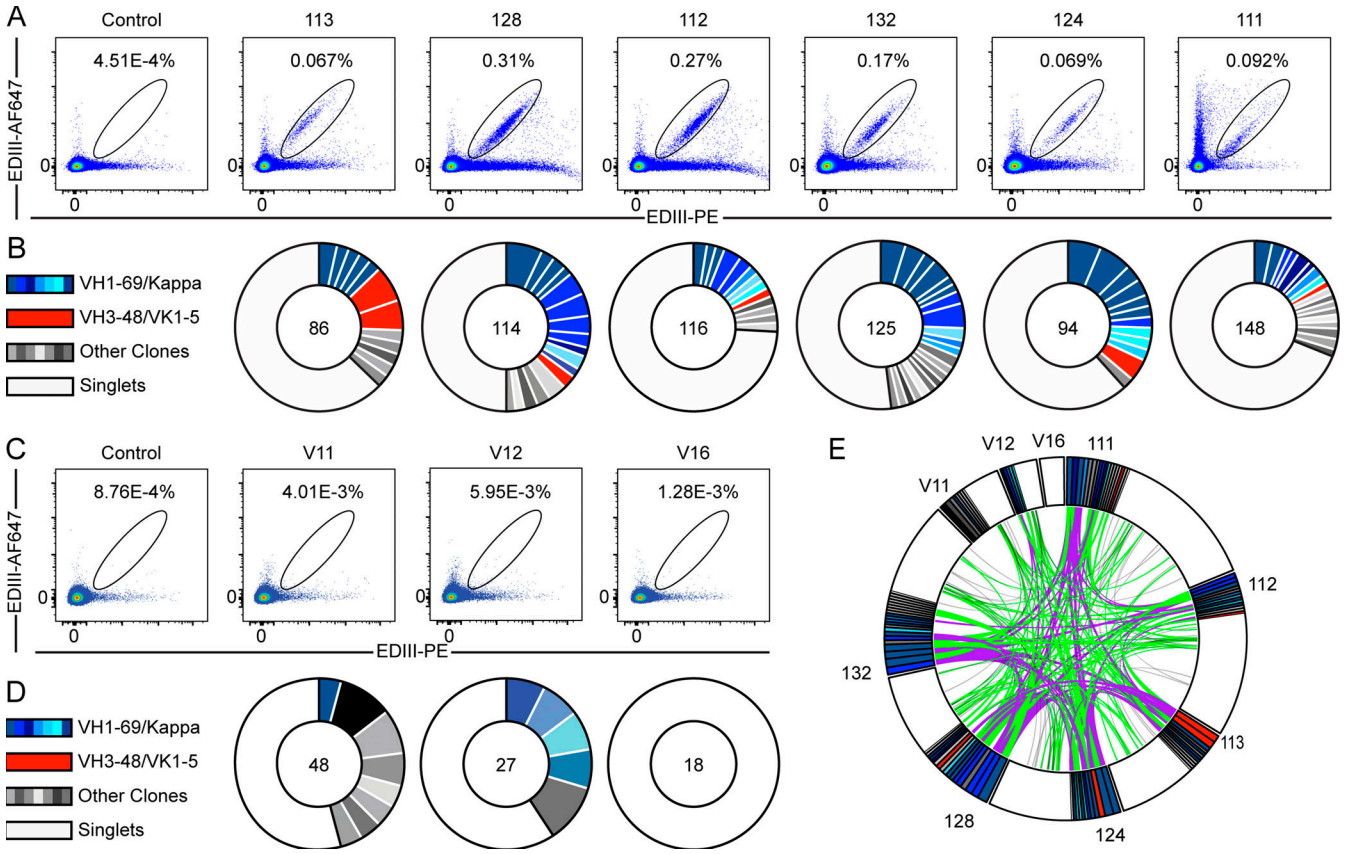

Figure 2. **Anti-TBEV antibodies from infected and vaccinated individuals. (A)** Identification of TBEV-specific B cells from infected donors. Representative flow cytometry plots showing B cells binding to AF647- and PE-labeled TBEV EDIII in one control and six TBEV-infected donors. Numbers indicate percentage of double-positive B cells. The gating strategy is shown in Fig. S2 A. **(B)** Clonal analysis of antibody sequences. Pie charts show the distribution of antibody sequences from infected donors. The number in the center represents the total number of antibody sequences obtained. Colored or gray pie slices correspond to clonally related sequences, with the size of the slice proportional to the number of sequences. All blue slices are IGVH1–69, and all red slices are IGVH3–48/IGVK1–5. White slices correspond to antibody sequences that are not part of a clone (singlets). **(C and D)** Same as in A and B, but for one healthy control and three vaccinated donors. **(E)** Antibody sequence relatedness. Circos plot shows sequences from all donors, with color-coding as in B and D. Connecting lines indicate antibodies that share IGH and IGL V and J genes. Purple, green, and gray lines connect related clones to each other, clones to singlets, and singlets to singlets, respectively. Related to Figs. S2 and S3, Table S2, and Table S3.

$Asp100_{HC}$ and $Trp94_{LC}$ into a cleft in the EDIII, making a salt bridge ($Asp100_{HC}$–$Lys311_{EDIII}$) and hydrogen bonds to the EDIII (Fig. 4 B). Crystal structures of T025 Fab in complex with $TBEV^{FE}$ EDIII and $TBEV^{Si}$ EDIII were similar to the T025-$TBEV^{WE}$ EDIII structure (root-mean-square deviations [RMSDs] = 0.54 Å for 518 Cα atoms and 0.26 Å for 525 Cα atoms, respectively), consistent with 100% sequence conservation between these three strains of virus in the EDIII epitope residues (Fig. S5).

We compared the T025 Fab–$TBEV^{WE}$ structure to a 3.9 Å cryo-EM structure of a mouse monoclonal antibody (19/1786) bound to the TBEV virion (Füzik et al., 2018). T025 and 19/1786 are related by <65% amino acid sequence identity in the V_HV_L and 47% in the CDRs, but structural alignment of the structures by the Cα atoms of the EDIIIs shows that the two antibodies recognize similar epitopes (Fig. 4 C) and adopt similar poses (Fig. 4 D). We can therefore use the lower-resolution cryo-EM structure to deduce details about how T025 binds to and neutralizes the virus. In addition to contacts with EDIII, 19/1786 interacts with either the EDI or EDII of a neighboring subunit (Füzik et al., 2018). This, taken together with the relatively low buried surface area on the EDIII by T025 (~600 Å^2 compared with a typical value of ~1,100 Å^2; Ramaraj et al., 2012), suggests that T025 also contacts neighboring domains on a native virion. It is also likely that, in common with recognition of virions by 19/1786, 120 of the 180 EDIIIs on the virion could be bound by T025.

Antibody T025 prevents and treats infection in mice

To determine whether anti-EDIII antibodies can protect against infection in vivo, we performed prophylaxis experiments in BALB/c mice. The mice received graded doses of T025 (100–0.1 µg per mouse) 24 h before challenge with 10^2 PFU TBEV (a lethal dose). All mice treated with the isotype control antibody died by day 10 (n = 6). In contrast, even the lowest dose of T025 was protective; all but 1 of the 24 mice receiving the antibody survived ($P < 0.0001$; Fig. 5 A). To test T025's potential for therapy, BALB/c mice were infected with 10^2 PFU TBEV and then injected with 30 µg T025 or isotype control 1, 3, or 5 d later (Fig. 5 B). All 12 control mice succumbed to the infection by day 13. In contrast,

Downloaded from http://rupress.org/jem/article-pdf/218/5/e20210236/1803798/jem_20210236.pdf by guest on 18 January 2024

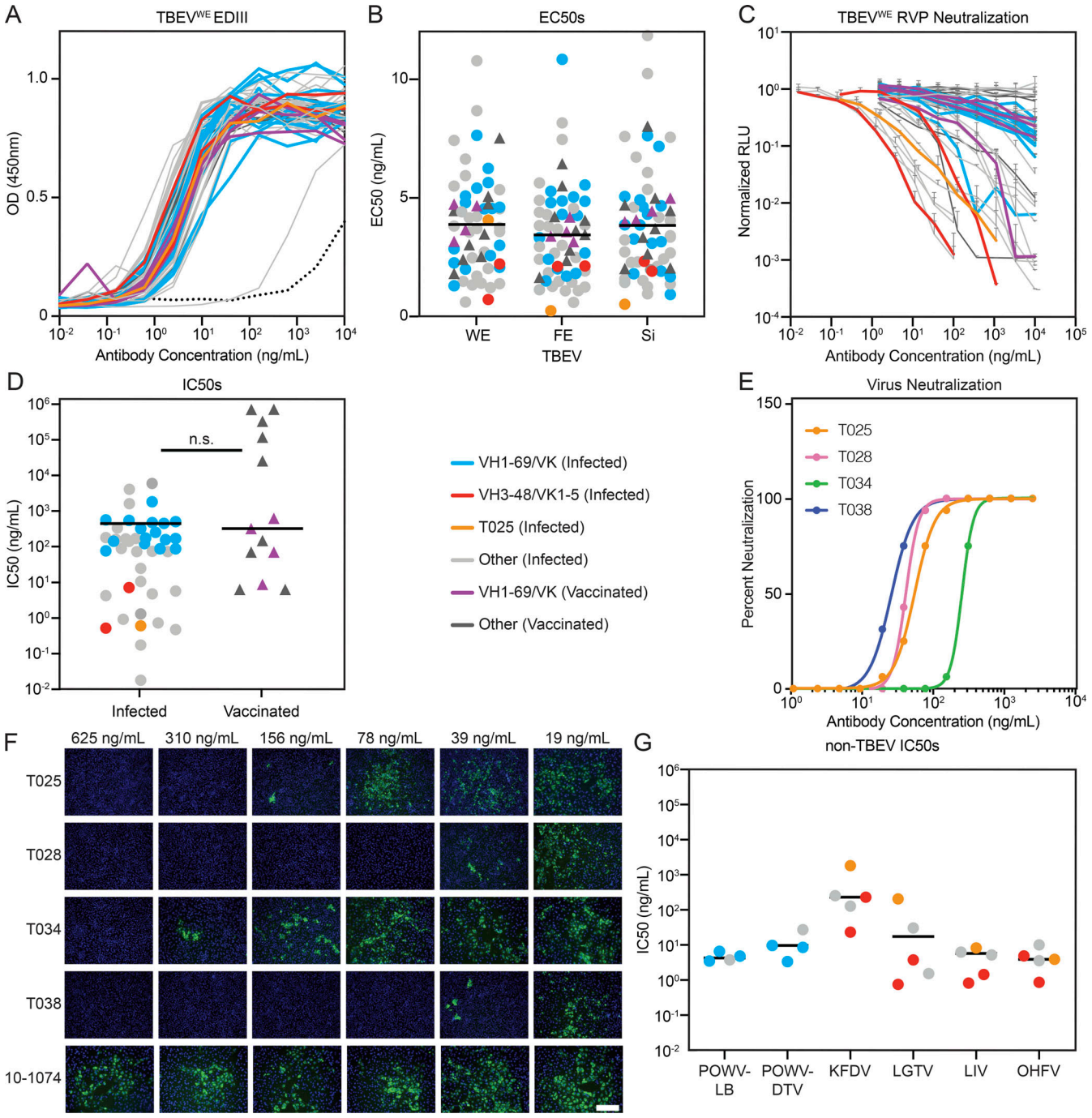

Figure 3. **Identification of potent and broadly cross-reactive monoclonal antibodies. (A)** TBEV^{WE} EDIII ELISA binding curves for 46 and 13 monoclonals from infected and vaccinated individuals, respectively. Data are representative of two experiments performed in singlicate. Dotted line is 10–1074 isotype control. **(B)** Dot plot summarizing average EC_{50} values for the antibodies in A to each of three TBEV subtype EDIIIs: TBEV^{WE}, TBEV^{FE}, and TBEV^{Si}. Average of two experiments. The horizontal lines indicate the mean value. **(C)** RVP neutralization curves for the antibodies in A normalized to no antibody control. Data are representative of two experiments, each performed in triplicate. Error bars indicate standard deviation. **(D)** Dot plot summarizing the average IC_{50} for TBEV^{WE} RVP neutralization by the antibodies as in C. Horizontal line indicates the mean IC_{50}. No statistical difference was found by two-tailed Mann–Whitney test. **(E and F)** TBEV neutralization in vitro. In E, curves represent virus neutralization by serially diluted antibodies. Representative of two independent experiments performed in octuplicate. In F, representative immunofluorescence microscopy images of PS cells infected in the presence of the indicated antibodies are shown. Green is viral antigen, and blue is cell nuclei. Scale bar indicates 200 µm. **(G)** Cross-neutralization by anti-TBEV antibodies. Graph shows IC_{50}s for selected antibodies against RVPs corresponding to POWV-LB, POWV-DTV, KFDV, LGTV, LIV, and OHFV. Average of two independent experiments performed in triplicate. Horizontal line indicates the mean IC_{50}. In A–D and G, blue and red indicate infected donor-derived IGVH1–69/kappa and IGVH3-48/IGVK1–5 antibodies, while purple indicates IGHV1–69/kappa antibodies from vaccinated individuals. Antibody T025 is shown in orange. In B, D, and G, circles and triangles correspond to antibodies derived from infected or vaccinated donors, respectively. Related to Fig. S4, Table S4, and Table S5.

Downloaded from http://rupress.org/jem/article-pdf/218/5/e20210236/1803798/jem_20210236.pdf by guest on 18 January 2024

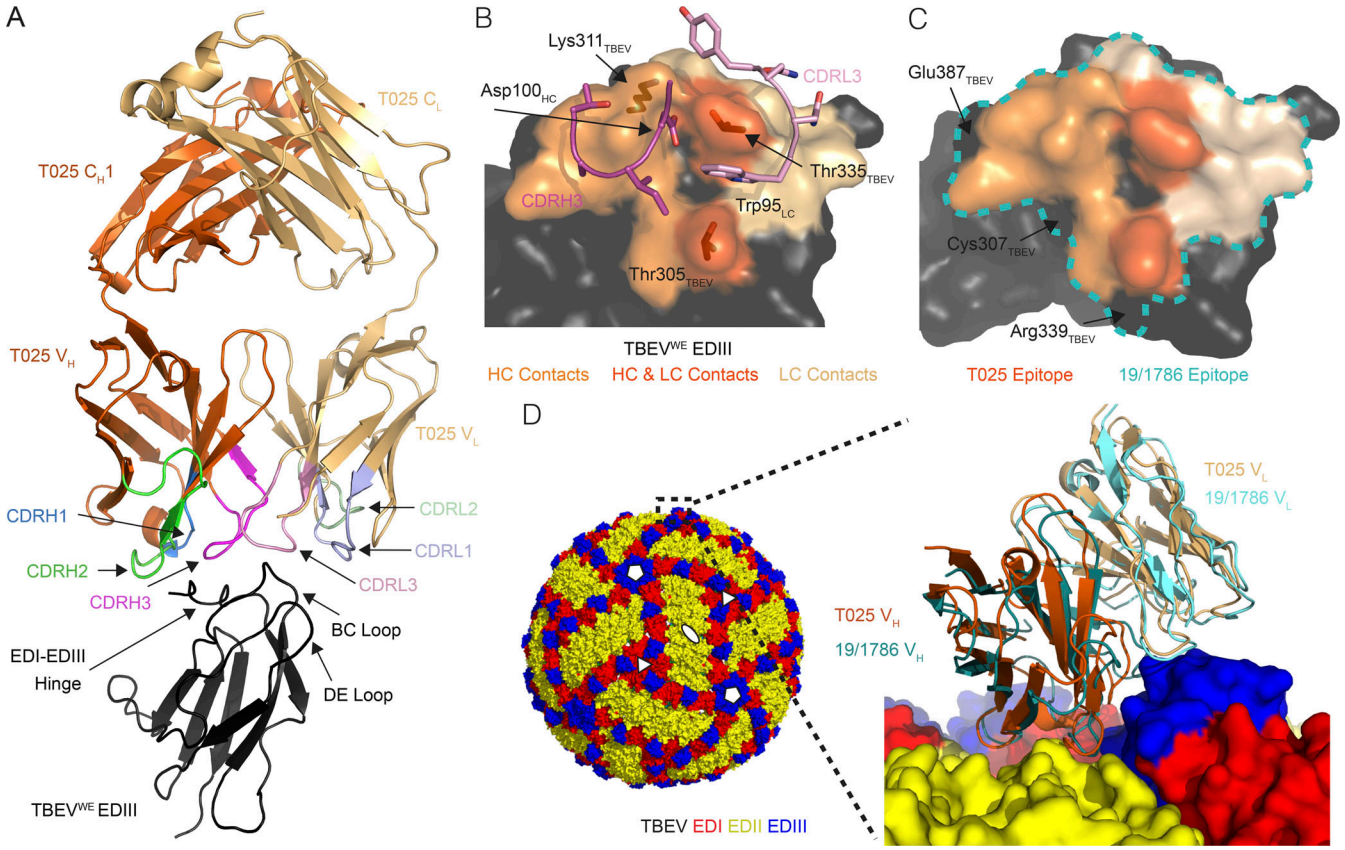

Figure 4. **T025 antibody recognizes a lateral ridge epitope on TBEV EDIII that is exposed on the mature virus structure. (A)** T025 recognition of the TBEV^{WE} EDIII. T025 interacts with the N-terminal region (EDI–EDIII hinge, the BC loop, and the DE loop) on TBEV^{WE} EDIII. **(B)** T025 epitope. TBEV^{WE} EDIII residues with an atom within 4 Å of a residue in the T025 Fab are highlighted on a surface representation of the EDIII antigen. CDRH3 and CDRL3 are shown as ribbon backbone with stick side chains. **(C)** T025 recognizes a similar epitope as the anti-TBEV mouse antibody 19/1786. The T025 epitope is shown in shades of orange; the 19/1786 epitope is outlined in a blue dashed line. Residues within the 19/1786 epitope, but not in the T025 epitope, are labeled. Epitopes are defined as residues that contain an atom within 4 Å of an atom in a residue on the antibody. **(D)** Surface representation of the cryo-EM structure of TBEV (PDB accession no. 5O6A) shown with fivefold, threefold, and twofold icosahedral symmetry operators at select vertices (left) with inset comparing binding poses of T025 and 19/1786 antibodies (right). Inset: Close-up of the indicated portion (dotted box) of the cryo-EM structure of the viral surface interacting with the 19/1786 V_HV_L domains (PDB accession no. 5O6V) with the E domains labeled in red, yellow, and blue and the V_HV_L domains in teal and cyan. The T025-TBEV^{WE} EDIII crystal structure was docked onto a virion EDIII adjacent to an icosahedral twofold symmetry axis after alignment of the EDIII domains (RMSD = 0.97 Å, 82 Ca atoms). The T025 V_HV_L binds EDIII with a similar pose as the 19/1786 V_HV_L. Related to Fig. S5 and Table S6.

12 out of 13 mice treated with T025 on day 1 and 4 out of 13 mice treated on day 3 after infection survived. All mice treated with T025 5 d after infection failed to respond. Thus T025, a broadly neutralizing human anti-TBEV antibody, is efficacious in prevention and early treatment of TBEV infection in BALB/c mice.

Discussion

Tick-borne flaviviruses can cause a fulminant encephalitis for which there is no effective therapy. This group of viruses are a growing public health concern in Europe, Asia, and North America. Among disease-causing tick-borne flaviviruses, TBEV is prevalent in Central Europe and Russia. Although there is a great deal of information on the polyclonal humoral immune response to TBEV (Albinsson et al., 2018; Holzmann, 2003; Matveeva et al., 1995; McAuley et al., 2017; Remoli et al., 2015), there is little or no understanding of the molecular nature of the neutralizing antibody response induced by natural infection or vaccination. We report on 776 antibodies obtained from memory B cells of six recovered and three vaccinated individuals, among which are several broad and potent neutralizers of tick-borne flaviviruses. The data provide insights into the human antibody response to TBEV and related pathogens, as well as mechanisms of antibody-induced neutralization. Finally, broad and potent neutralizing human monoclonal antibodies are highly effective for protection and therapy in vivo and have significant potential for clinical use.

Human neutralizing antibody responses to pathogens frequently converge on the same IGV genes. Examples include neutralizing antibodies to HIV-1, influenza, Zika, hepatitis B, and SARS-CoV-2 viruses (Robbiani et al., 2017; Robbiani et al., 2020; Scheid et al., 2011; Tiller et al., 2007; Wang et al., 2020; West et al., 2012). Antibodies to the EDIII of TBEV produced by different individuals show strong homology that, like SARS-CoV-2 antibodies, extends beyond IGV heavy and light chain gene pairing and includes the CDR3 regions.

Downloaded from http://rupress.org/jem/article-pdf/218/5/e20210236/1803798/jem_20210236.pdf by guest on 18 January 2024

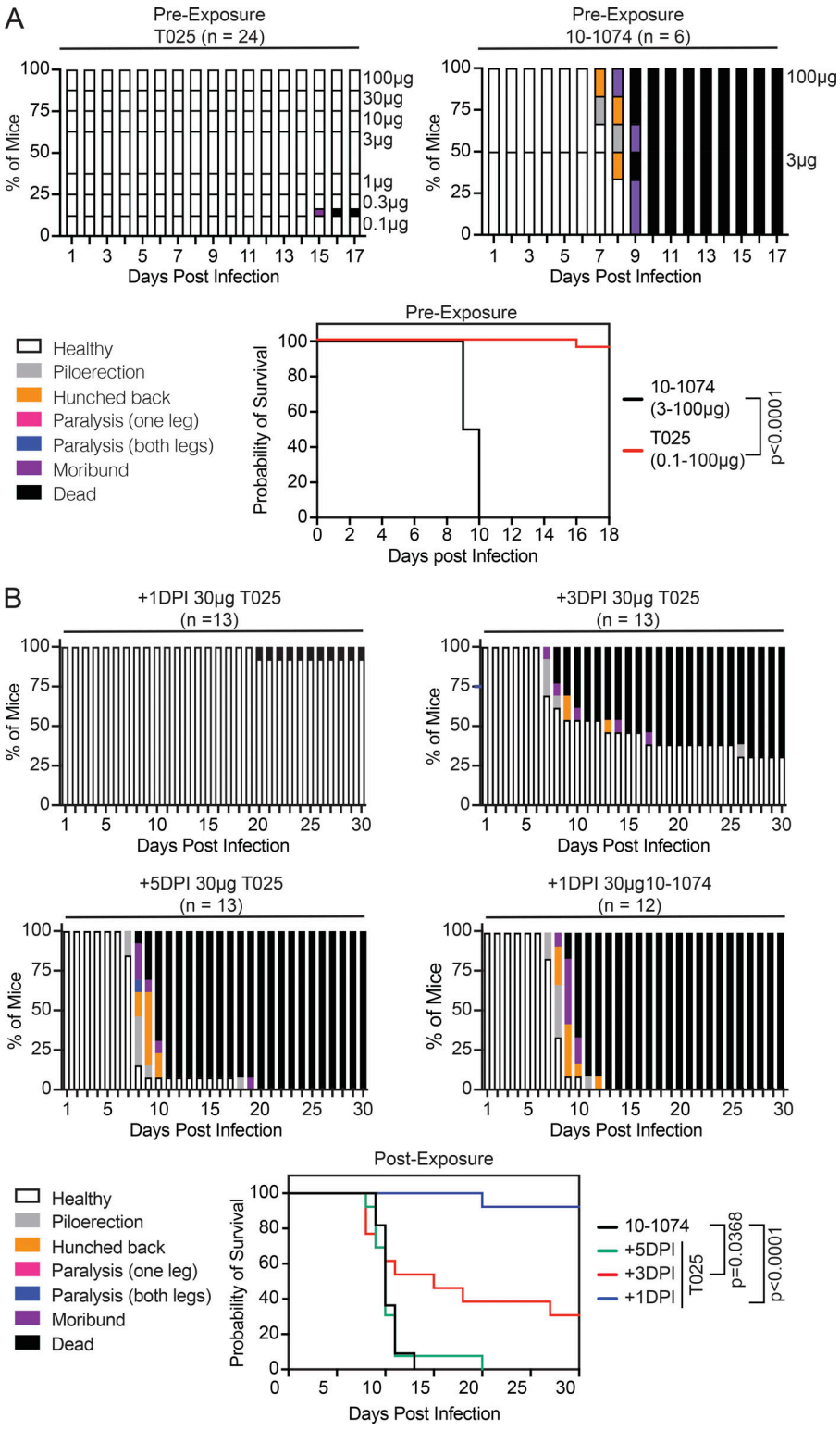

Figure 5. **Prevention and therapy with T025.** **(A)** T025 is efficacious in preexposure prophylaxis. Mice were treated with T025 or 10–1074 (isotype control) 24 h before infection with a lethal dose of TBEV-Hypr. Top: Histogram shows disease score over time. Antibody dose is indicated on the right. Two independent experiments were combined, with three mice per group. Bottom: Kaplan–Meier survival curve. The P value was calculated with the Mantel–Cox test ($P < 0.0001$). **(B)** T025 protects mice when administered after infection. Mice were treated with 30 µg T025 or control 10–1074 at 1, 3, or 5 d post infection (DPI). Three experiments were combined, with six or seven mice per group; $P < 0.0001$ for +1 DPI, $P = 0.0368$ for +3 DPI, and no significant difference for +5 DPI by Mantel–Cox test.

Among the neutralizing antibodies to TBEV, VH1–69 and VH3–48 were recurrent in multiple donors. VH1–69 was paired with a variety of light chain genes to produce neutralizing antibodies that were found among vaccinees and recovered individuals. This group of antibodies varied broadly in neutralizing activity with IC_{50}s ranging from 12–1,180 ng/ml (geometric mean, 186.2 ng/ml). VH1–69 antibodies are highly represented in the human repertoire and are also common among broadly neutralizing antibodies to influenza, hepatitis C, and HIV-1 viruses (Chen et al., 2019). Anti-TBEV VH3–48 antibodies differed from VH1–69 in that they were always paired with the same light chain, VK1–5. VH3–48 antibodies were also more potent than VH1–69, with IC_{50}s ranging from 0.5 to 7.3 ng/ml (geometric mean, 2 ng/ml), and they were only found in

Downloaded from http://rupress.org/jem/article-pdf/218/5/e20210236/1803798/jem_20210236.pdf by guest on 18 January 2024

convalescent individuals. The absence of this class of potent antibodies in the vaccinees examined is consistent with the lower levels of serum neutralizing potency in this group. Finally, VH3–48 antibodies are also potent neutralizers of several related tick-borne flaviviruses including KFDV, LGTV, LIV, and OHFV, with IC_{50}s of 1–36 ng/ml.

Antibodies to a number of different flaviviruses, including dengue and Zika virus, can be protective if administered before and even after infection (Robbiani et al., 2017; Xu et al., 2017). In Russia and Kazakhstan, administration of TBEV hyperimmune plasma Ig is recommended for postexposure prophylaxis for individuals that present within 3 d of a tick bite (Pen'evskaia and Rudakov, 2010; Russian Ministry of Health, 2008). The efficacy of this intervention may vary from batch to batch of donor plasma Ig (Rabel et al., 2012; Ruzek et al., 2019), and its use was discontinued in some countries after a small number of adverse events and concerns about the possibility of antibody-dependent enhancement of disease (Arras et al., 1996; Kluger et al., 1995; Waldvogel et al., 1996). Mouse monoclonal antibodies can also protect against TBEV but have not been tested in the clinic (Baykov et al., 2014; Levanov et al., 2010; Matveev et al., 2020). Our experiments extend previous work by uncovering human monoclonal antibodies that prevent infection in mice even when administered at doses as low as ∼0.005 mg/kg. Notably, these antibodies also suppress disease in mice, even when administered 3 d after infection at a dose of ∼1.5 mg/kg.

Antibodies against EDIII are often among the most potent raised during flavivirus infection (Beasley and Barrett, 2002; Beltramello et al., 2010; Crill and Roehrig, 2001; Screaton et al., 2015; Sun et al., 2017). The broad and potent anti-TBEV antibody T025 recognizes a lateral ridge epitope on EDIII that is also targeted by antibodies raised against other flaviviruses (Edeling et al., 2014; Füzik et al., 2018; Nybakken et al., 2005; Renner et al., 2018; Robbiani et al., 2017; Zhao et al., 2020). Several human antibodies against the lateral ridge of EDIII have been previously characterized, including Z021 isolated from a convalescent Zika donor, which recognizes a similar epitope and has an angle of approach similar to T025 (Keeffe et al., 2018). These results suggest a common mechanism for potent neutralization of flaviviruses. Targeting this epitope likely interferes with the structural rearrangement necessary for fusion, preventing infection (Füzik et al., 2018; Nybakken et al., 2005; Renner et al., 2018; Thompson et al., 2009). Although anti-EDIII antibodies can be potently neutralizing, antibodies against the EDIII in humans constitute only a small fraction of the immune response (Beltramello et al., 2010; Lai et al., 2008; Wahala et al., 2009), suggesting that a targeted vaccine strategy focusing on EDIII could be beneficial.

While most antibodies to flavivirus EDIII are thought to be virus specific (Crill and Roehrig, 2001; Pierson et al., 2008; Roehrig, 2003; Stettler et al., 2016), T025 is a potent neutralizer of not only TBEV but also several other tick-borne flaviviruses. The pairwise sequence identity of the EDIII epitope of TBEV to predicted epitopes in LGTV, LIV, and OHMV EDIIIs is high (differences of 1–2 amino acids), and the residues that differ have similar biochemical properties (e.g., threonine to serine). The exception is KFDV, which is sensitive to T025 but differs in sequence to TBEV in the T025 epitope on the EDIII. Contacts made outside of the EDIII may also contribute to the sensitivity of KDFV to T025. Powassan virus contains an amino acid insertion in the BC loop of the EDIII compared with the TBEV EDIII, which likely prevents binding of T025 and therefore is insensitive to T025 neutralization.

Available TBEV vaccines were developed over 30 yr ago and consist of inactivated virus grown on chick embryo cells. Vaccination is TBEV specific, requires priming and two boosts, and results in 90–100% seroconversion depending on the vaccine used (Loew-Baselli et al., 2009; Maikova et al., 2019; Vorovitch et al., 2019). Additional boosts are recommended every 3–5 yr for the lifetime of the individual. The existence of broad and potent VH3–48 antibodies suggests that next-generation vaccines specifically designed to target the epitope recognized by these antibodies might be universally effective against TBEV, KFDV, LGTV, LIV, and OHFV. Finally, potent human antibodies with broad activity against tick-borne flaviviruses have significant potential for clinical use in individuals who are at high risk and do not respond to the vaccine, as well as for therapy in the early stages of infection.

Materials and methods

Human subjects and clinical information

Samples of peripheral blood were obtained upon consent from individuals previously hospitalized with confirmed TBEV infection or individuals previously vaccinated against TBEV in České Budějovice, Czech Republic, under protocols approved by the ethical committees of the Hospital in České Budějovice (approval no. 103/19), the Biology Center of the Czech Academy of Sciences (approval no. 1/2018), and The Rockefeller University (IRB DRO-0984). Clinical data were obtained at the treating hospital, and severity of disease was evaluated according to the following scale: mild, flu-like symptoms with meningeal irritation defined as meningitis, characterized by fever, fatigue, nausea, headache, back pain, arthralgia/myalgia and neck or back stiffness; moderate, previous symptoms together with tremor, vertigo, somnolence, and photophobia defined as meningoencephalitis; severe, prolonged neurological consequences including ataxia, titubation, altered mental status, memory loss, quantitative disturbance of consciousness, and palsy revealed as encephalitis, encephalomyelitis, or encephalomyeloradiculitis (Bogovic and Strle, 2015; Ruzek et al., 2019).

Blood samples processing and storage

Peripheral blood mononuclear cells (PBMCs) were obtained by gradient centrifugation using Ficoll and stored in liquid nitrogen in freezing media (90% FCS and 10% DMSO). Prior to experiments, aliquots of sera (from infected, vaccinated, and random blood bank donors) were heat-inactivated at 56°C for 1 h and then stored at 4°C.

Protein expression and purification

EDIII antigens were expressed in *Escherichia coli* and purified from inclusion bodies as previously reported (Robbiani et al., 2017; Sapparapu et al., 2016). Expression vectors containing

Downloaded from http://rupress.org/jem/article-pdf/218/5/e20210236/1803798/jem_20210236.pdf by guest on 18 January 2024

codon-optimized sequences encoding residues 299–397 for TBEV strain Neudoerfl ($TBEV^{WE}$; NC_001672.1) or 301–397 for strains Sofjin ($TBEV^{FE}$; UniProtKB accession no. P07720) and Vasilchenko ($TBEV^{Si}$; AF069066) were used to produce untagged EDIII proteins or EDIII proteins containing a C-terminal 6XHis-Avitag. Constructs encoding untagged EDIIIs of other tick-borne flaviviruses were constructed similarly (POWV strain LB, GenBank accession nos. L06436.1; POWV isolate DTV, HM440561.1; KFDV strain W-377, JF416960.1; LGTV strain TP21-636, NC_003690.1; LIV isolate LI3/1, KP144331.1; OHFV strain Bogoluvovska, NC_005062). Expression plasmids were transformed into BL21(DE3) *E. coli* and induced with 1 mM isopropyl β-D-1-thiogalactopyranoside at 37°C for 4 h. The cells were lysed and the insoluble fraction containing inclusion bodies was solubilized and refolded in 400 mM L-arginine, 100 mM Tris-base, pH 8.0, 2 mM EDTA, 0.2 mM phenyl-methylsulfonyl fluoride, 5 mM reduced and 0.5 mM oxidized glutathione, and 10% glycerol at 4°C. Refolded protein was purified by size exclusion chromatography (Cytiva; Superdex 75) in 20 mM Tris, pH 8.0, 150 mM NaCl, and 0.02% NaN_3. EDIIIs were concentrated to 10–20 mg/ml.

T025 Fabs for structural studies were produced and purified as described in previous studies (Keeffe et al., 2018; Robbiani et al., 2017; Robbiani et al., 2020; Wang et al., 2020). Briefly, Fabs containing a 6XHis purification tag at the C terminus of the HC were expressed by transiently transfecting Expi293 cells (Life Technologies) with appropriate heavy and light chain plasmids. His-tagged Fabs were purified from expression supernatants using Ni-nitrilotriacetic acid affinity chromatography (Cytiva) followed by size exclusion chromatography (Cytiva; Superdex 200) in 20 mM Tris, pH 8.0, 150 mM NaCl, and 0.02% NaN_3. Fabs were concentrated to ∼15 mg/ml.

Sequence analysis

Antibody sequences were analyzed as described previously (Robbiani et al., 2020); briefly, sequences were trimmed and annotated using Igblastn v.1.14.0 (Ye et al., 2013) and Change-O toolkit v.0.4.5 (Gupta et al., 2015). Sequences from the same cell were paired and assigned clonotypes based on V and J genes using in-house R and Perl scripts (available on GitHub; https://github.com/stratust/igpipeline). Nucleotide somatic hypermutation and CDR3 length were also analyzed using in-house R and Perl scripts, as described previously (Robbiani et al., 2020); hypermutation analysis was based on the closest germlines in Igblastn. Hydrophobicity GRAVY (grand average of hydropathy) scores were calculated using Guy H.R. Hydrophobicity scale (Guy, 1985; Kyte and Doolittle, 1982) and R package Peptides (https://journal.r-project.org/archive/2015/RJ-2015-001/RJ-2015-001.pdf), based on 776 IGH CDR3 sequences from this study and 22,654,256 IGH CDR3 sequences from public databases of memory B cell receptor sequences (DeWitt et al., 2016). Distribution was determined using the Shapiro–Wilk test with all CDR3 sequence GRAVY scores from this study and 5,000 randomly selected GRAVY scores from the public database. The Wilcoxon nonparametric test was used to test for significant difference in hydrophobicity.

Frequency distributions of V genes in anti-TBEV antibodies from six infected donors were compared with Sequence Read Archive accession no. SRP010970 (https://trace.ncbi.nlm.nih.gov/Traces/sra/?study=SRP010970; Rubelt et al., 2012). V gene assignments were based on the above-described analysis, and frequencies were calculated for six infected donors using sequences with unique CDR3s. Statistical significance was determined using two-tailed *t* tests with unequal variances. Sequence logos were generated from left-aligned CDR3 sequences from each antibody set using WebLogo (Crooks et al., 2004).

Protein biotinylation

Avi-tagged $TBEV^{FE}$ EDIII was biotinylated using the Biotin-Protein Ligase BIRA kit according to the manufacturer's instructions (Avidity) and conjugated to streptavidin-PE (BD Biosciences; 554061) and streptavidin-Alexa Fluor 647 (BioLegend; 405237). Ovalbumin (Sigma-Aldrich; A5503-1G) was biotinylated using the EZ Sulfo-NHS-LC-Biotinylation kit according to the manufacturer's instructions (Thermo Fisher Scientific; A39257) and conjugated to streptavidin BV711 (BD Biosciences; 563262). Biotinylation was confirmed by ELISA before use in flow cytometry.

Single-cell sorting

PBMCs from sample 111 were enriched for B cells via positive selection using CD19 microbeads (Miltenyi Biotec; 130–050-301). PBMCs from all other donors were enriched for B cells by negative selection (Miltenyi Biotec; 130–101-638). All selection protocols were performed according to the manufacturer's instructions. Enriched B cells were incubated for 30 min on ice in FACS buffer (1× PBS, 2% calf serum, 1 mM EDTA) with fluorophore-labeled EDIII and ovalbumin, and in the presence of anti-human antibodies anti-CD3-APC-eFluro 780 (Invitrogen; 47–0037-41), anti-CD8-APC-eFluro 780 (Invitrogen; 47–0086-42), anti-CD14-APC-eFluro 780 (Invitrogen; 47–0149-42), anti-CD16-APC-eFluro 780 (Invitrogen; 47–0168-41), anti-CD20-PECy7 (BD Biosciences; 335793), and Zombie NIR (BioLegend; 423105). Single $CD3^-CD8^-CD14^-CD16^-ZombieNIR^-CD20^+Ova^-EDIII\text{-}PE^+EDIII\text{-}AF647^+$ B cells were sorted using a FACS Aria III (Becton Dickinson) into individual wells of 96-well plates. Each well contained 4 µl of a lysis buffer comprising 0.5× PBS, 10 mM DTT, and 3,000 U/ml RNasin Ribonuclease Inhibitors (Promega; N2615). Sorted cells were snap-frozen on dry ice and then stored at −80°C. Antibody sequences are derived from memory B cells because they originate from small $CD20^+$ cells, and the antibody genes were PCR amplified using IgG-specific primers.

Antibody sequencing, cloning, and expression

RNA from single cells was reverse transcribed using SuperScript III Reverse transcription (Invitrogen; 18080–044). The resulting cDNA was stored at −20°C until amplification of the variable Ig heavy (IGH), Ig light (IGL), and Ig kappa (IGK) genes by nested PCR followed by Sanger sequencing. Amplicons from the first PCR reaction were used as template for nested PCR-amplification followed by sequence- and ligation-independent cloning into antibody expression vectors as previously described (Robbiani et al., 2020). Recombinant monoclonal antibodies were produced and purified as previously detailed (Klein et al., 2014).

Downloaded from http://rupress.org/jem/article-pdf/218/5/e20210236/1803798/jem_20210236.pdf by guest on 18 January 2024

Plasmids for the production of RVP

A West Nile virus subgenomic replicon-expressing plasmid encoding Renilla luciferase (pWNVII-Rep-REN-IB) and a ZIKV CprME expression plasmid had previously been obtained from Ted Pierson (National Institutes of Health, Bethesda, MD; Pierson et al., 2006; Robbiani et al., 2017). The ZIKV CprME expression plasmid was manipulated by restriction enzyme digestion and ligation to express the CprME of other flaviviruses as follows.

TBEV

Synthetic DNA with CprME coding sequence (flanked at the 5′ by the polylinker and Kozak sequence 5′-GGAATTCGCGGCCGC CTCAGG-3′ and at the 3′ by the stop codons and polylinker 5′-TAATAGTTAATTAACTCGAGCCGCGG-3′; "CprME flanked") corresponding to TBEV, Western European subtype strain Neudoerfl (GenBank accession no. NC_001672), was amplified with primers DFRp1532 (5′-GGAATTCGCGGCCGCCTCAGG-3′) and DFRp1533 (5′-GCGGCTCGAGTTAATTAA-3′) before cloning at the NotI and PacI sites of plasmid pPOWV-LB-CprME (see below), resulting in pTBEV-WE-CprME.

POWV-LB

Synthetic DNA containing the CprME sequence (underlined) of POWV-LB strain (GenBank accession no. L06436.1 with six synonymous changes (in lowercase and bold) to reduce complexity; 5′-CTACTTGGCAGTACATCTACGTATTAGTCATCGCTA TTACCATGGTGATGCGGTTTTGGCAGTACATCAATGGGCGTG GATAGCGGTTTGACTCACGGGGATTTCCAAGTCTCCACCCCA TTGACGTCAATGGGAGTTTGTTTTGGCACCAAAATCAACGGG ACTTTCCAAAATGTCGTAACAACTCCGCCCCATTGACGCAAA TGGGCGGTAGGCGTGTACGGTGGGAGGTCTATATAAGCAGAG CTCTCTGGCTAACTAGAGAACC**C**ACTGCTTACTGGCTTATCGAA ATTAATACGACTCACTATAGGGAGACCCAAGCTGGCTAGTTA AGCTATCAACAAGGAATTCGCGGCCGCCAGGCTATGATGACC ACTTCTAAAGGAAAGGGGGGCGGTCCCCCTAGGCGCAAGCTT AAAGTGACCGCAAATAAGTCGCGACCAGCAACGAGCCCAATG CCAAAGGGCTTCGTGCTGTCGCGCATGCTGGGGATTCTTTGG CACGCCGTGACAGGCACGGCCAGACCCCCAGTGCTGAAAATG TTCTGGAAAACGGTACCACTGCGCCAGGCGGAGGCTGTTCTG AAGAAGATAAAGAGAGTTATCGGGAACTTGATGCAGAGCCTT CACATGAGAGGGCGTCGCAGGTCAGGTGTGGACTGGACTTGG ATTTTTTTGACGATGGCGTTGATGACCATGGCCATGGCAACC ACCATCCACCGGGACAGGGAAGGATACATGGTTATGCGGGCC AGTGGAAGGGACGCTGCAAGCCAGGTCAGGGTACAAAACGGA ACGTGCGTCATCCTGGCAACAGACATGGGAGAGTGGTGTGAA GATTCAATCACCTACTCTTGCGTCACGATTGACCAGGAGGAA GAACCCGTTGACGTGGACTGCTTCTGCCGAGGTGTTGATAGG GTTAAGTTAGAGTATGGACGCTGTGGAAGGCAAGCTGGATCT AGGGGGAAAAGGTCTGTGGTCATTCCAACACATGCACAAAAA GACATGGTCGGGCGAGGTCATGCATGGCTTAAAGGTGACAAT ATTCGAGATCATGTCACCCGAGTCGAGGGCTGGATGTGGAAG AACAAGCTTCTAACTGCCGCCATTGTGGCCTTGGCTTGGCTC ATGGTTGATAGTTGGATGGCCAGAGTGACTGTCATCCTCTTG GCGTTGAGTCTAGGGCCAGTGTACGCCACGAGGTGCACGCAT CTTGAGAACAGAGATTTTGTGACAGGAACTCAAGGGACCACC AGAGTGTCCCTAGTTTTGGAACTTGGAGGCTGCGTGACCATC ACAGCTGAGGGCAAGCCATCCATTGATGTATGGCTCGAAGAC ATTTTTCAGGAAAGCCCGGCTGAAACCAGAGAATACTGCCTG CACGCCAAATTGACCAACACAAAAGTGGAGGCTCGCTGTCCA ACCACTGGACCGGCGACACTTCCGGAGGAGCATCAGGCTAAT ATGGTGTGCAAGAGAGACCAAAGCGACCGTGGATGGGGAAAC CACTG**t**GG**a**TT**c**TT**c**GGGAAGGGCAGTATAGTGGCTTGTGCA AAGTTTGAATGCGAGGAAGCAAAAAAAGCTGTGGGCCACGTC TATGACTCCACAAAGATCACGTATGTTGTCAAGGTTGAGCCC CACACAGGGGATTACTTGGCTGCAAATGAGACCAATTCAAAC AGGAAATCAGCACAGTTTACGGTGGCATCCGAGAAAGTGATC CTGCGGCTCGGCGACTATGGAGATGTGTCGCTGACGTGTAAA GTGGCAAGTGGGATTGATGTCGCCCAAACTGTGGTGATGTCA CTCGACAGCAGCAAGGACCACCTGCCTTCTGCATGGCAAGTG CACCGTGACTGGTTTGAGGACTTGGCGCTGCCCTGGAAACAC AAGGACAACCAAGATTGGAACAGTGTGGAGAAACTTGTGGAA TTTGGACCACCACATGCTGTGAAAATGGATGTTTTCAATCTG GGGGACCAGACGGCTGTGCTGCTCAAATCACTGGCAGGAGTT CCGCTGGCCAGTGTGGAGGGCCAGAAATACCACCTGAAAAGC GGCCATGTTACTTGTGATGTGGGACTGGAAAAGCTGAAACTG AAAGGCACAACCTACTCCATGTGTGACAAAGCAAAGTTCAAA TGGAAGAGAGTTCCTGTGGACAGCGGCCATGACACAGTAGTC ATGGAGGTATCATACACAGGAAGCGACAAGCCATGTCGGATC CCGGTGCGGGCTGTGGCACATGGTGTCCCAGCGGTTAATGTA GCCATGCTCATAACCCCCAATCCAACCATTGAAACAAATGGT GGCGGATTCATAGAAATGCAGCTGCCACCAGGGGATAACATC ATCTATGTGGGAGACCTTAGCCAGCAGTGGTTTCAGAAAGGC AGTACCATTGGTAGAATGTTTGAAAAAACCCGCAGGGGATTG GAAAGGCTCTCTGTGGTTGGAGAACATGCATGGGACTTTGGC TCAGTAGGCGGGGTACTGTCTTCTGTGGGGAAGGCAATCCAC ACGGTGCTGGGGGGAGCTTTCAACACCCTTTTTGG**t**GG**t**GTT GGATTCATCCCTAAGATGCTGCTGGGGGTTGCTCTGGTCTGG TTGGGACTAAATGCCAGGAATCCAACGATGTCCATGACGTTT CTTGCTGTGGGGGCTTTGACACTGATGATGACAATGGGAGTT GGGGCATAATAGTTAATTAACTCGAGCCGCGGTTCGAAGGTA AGCCT-3′) was PCR amplified with primers DFRp1511 (5′-ATC TACGTATTAGTCATCGCTATTA-3′) and DFRp1514 (5′-ACCGCG GCTCGAGTTAATTAA-3′) and cloned at the Eco105I and SacII sites of plasmid pZIKV-HPF-CprME (Pierson et al., 2006; Robbiani et al., 2017), resulting in pPOWV-LB-CprME.

POWV-DTV

A three-piece assembly PCR strategy was used. DNA upstream of the CMV promoter in pZIKV-HFP-CprME to just downstream of the beginning of the C-encoding region was PCR amplified with primers RU-O-24611 (5′-CTTGACCGACAATTGCATGAAG-3′) and RU-O-26690 (5′-**CTTTCCTTTAGAAGTAGTCACCAT**AGC CTGCTTTTTTTGTACAAAC-3′), resulting in a fragment fusing the CMV promoter with POWV-DTV C-encoding sequences (bolded in primer RU-O-26690). Using as template DTVp1 (Kenney et al., 2018), kindly provided by Aaron Brault (Centers for Disease Control and Prevention, Fort Collins, CO) and based on the Spooner strain of DTV, a fragment overlapping with the CMV promoter–DTV C fusion to the region just downstream of a SacII site within DTV genome was generated by PCR using oligos RU-O-26689 (5′-GTTTGTACAAAAAAGCAGGCT**ATGGTGACTACT TCTAAAGGAAAG**-3′) and RU-O-26711 (5′-GTTTCCCCATCC**T** C**TA**TCGCTCTG-3′), with bolded nucleotides indicating

Downloaded from http://rupress.org/jem/article-pdf/218/5/e20210236/1803798/jem_20210236.pdf by guest on 18 January 2024

synonymous mutations introduced to ablate the SacII site. DNA was amplified using DTVp1 as template and oligos RU-O-26710 (5′-CAGAGCGA**TA**G**A**GGATGGGGAAAC-3′; bolded nucleotides indicate synonymous mutations) and RU-O-26688 (5′-TTCGAA CCGCGGCTGGGTCCTATTA**TGCTCCGACTCCCATTGTCATCAT C**-3′) to generate a fragment overlapping the killed SacII site to the end of the E protein coding region followed by a SacII site. The three DNA fragments were annealed, extended and then PCR amplified using primers RU-O-24611 and RU-O-26688. The resulting DNA fragment was digested with SnaBI and SacII and cloned into similarly digested pZIKV-HPF-CprME to generate pPOWV-DTV-CprME.

KFDV

Synthetic DNA with the CprME-flanked sequence of KFDV, strain W-377 (GenBank accession no. JF416960.1), was amplified with primers DFRp1532 and DFRp1533 before cloning at the NotI and PacI sites of plasmid pPOWV-LB-CprME (see above), resulting in pKFDV-W-377-CprME.

LGTV

The CprME of LGTV, isolate TP21-636, was amplified from a plasmid kindly provided by Dr. Sonja Best (Rocky Mountain Laboratories of National Institutes of Health/National Institute of Allergy and Infectious Diseases, Hamilton, MT) with primers DFRp1563 (5′-GGAATTCGCGGCCGCCTCAGGATGGCCGGGAAG GCCGTTCTA-3′) and DFRp1566 (5′-CCGCGGCTCGAGTTAATT AACTATTAGGCTCCAACCCCCAGAGTCAT-3′) before cloning at the NotI and PacI sites of plasmid pPOWV-LB-CprME, resulting in pLGTV-TP21-636-CprME. There are two nucleotide mutations from GenBank accession no. NC_003690 (A590G and A1893C).

LIV

Synthetic DNA with the CprME-flanked sequence of LIV, isolate LI3/1 (GenBank accession no. KP144331), was amplified with primers DFRp1532 and DFRp1533 before cloning at the NotI and PacI sites of plasmid pPOWV-LB-CprME, resulting in pLIV-LI3/1-CprME.

OHFV

Synthetic DNA with the CprME-flanked sequence of OHFV, strain Bogoluvovska (GenBank accession no. NC_005062), was amplified with primers DFRp1532 and DFRp1533 before cloning at the NotI and PacI sites of plasmid pPOWV-LB-CprME, resulting in pOHFV-CprME.

To confirm the absence of PCR-induced errors, all PCR-derived regions were sequenced in the final plasmids.

RVP production

RVPs were produced by cotransfecting 1 µg pWNVII-Rep-REN-IB plasmid with 3 µg of the flavivirus CprME plasmid of choice into the permissive cell line Lenti-X 293T using Lipofectamine 2000 (Invitrogen; 1166803) according to the manufacturer's instructions. Cells were seeded 24 h previously at 10^6 cells/well in collagen-coated 6-well plates. Following transfection and 6 h incubation at 37°C, excess DNA–lipid complexes were removed by aspiration and the media replaced with DMEM (Gibco) containing 20 mM Hepes and 10% FBS. For the next 72 h, in 24-h intervals, RVP-containing supernatants were harvested and filtered through a 0.45-µm filter and frozen at −80°C, and media were replaced with DMEM containing 20 mM Hepes and 10% FBS. Frozen RVPs were later thawed and titrated on Huh-7.5 cells to determine the dilution of RVPs at which cells express 10^6 relative light units in the absence of sera or antibody.

RVP neutralization assays

96-well plates were seeded with 7,500 Huh-7.5 cells/well in 50 µl DMEM (Gibco) supplemented with 10% FBS and 1% non-essential amino acids. After 24 h, 100 µl diluted RVPs were combined with 100 µl diluted sera or antibody, incubated for 1 h at 37°C, and then 50 µl of the mix were added in triplicate to the plated cells. RVPs are diluted appropriately in BA-1 diluent (Medium 199 [Lonza] supplemented with 1% BSA and 100 units/ml penicillin/streptomycin) to achieve the desired relative light unit expression. After an additional 24 h of incubation at 37°C, media was aspirated off the cells, replaced with 35 µl lysis buffer (Promega; E2810), and the plates were frozen at −80°C. 15 µl of the subsequently thawed lysis buffer was used for Renilla luciferase expression measurement using the Renilla Luciferase Assay System (Promega; E2810). Sera were either diluted to 1:600,000 final concentration for TBEV RVP neutralization screening or serially diluted to generate curves. Recombinant monoclonal antibodies were used at 10 µg/ml final concentration and serially diluted 1:3 for neutralization assays. NT_{50} and IC_{50} were determined by nonlinear regression analysis using Prism software (GraphPad). In the cross-neutralization screening against the panel of flavivirus RVPs, recombinant antibodies were assayed at 1 µg/ml final concentration using the protocol described above, and the results were compared with no antibody control.

ELISA assays

Binding of serum IgG or recombinant IgG antibodies to EDIII proteins was measured by standard ELISA. High-binding 96-well plates (Costar; 07–200-721) were coated overnight with 250 ng of the EDIII protein in PBS per well at room temperature; plates were then blocked with 0.1 mM EDTA, 0.05% Tween, and 2% BSA in PBS for 2 h at room temperature. Samples were diluted in PBS-T, added to plates, and incubated for an additional 1 h at room temperature. Secondary goat anti-human-IgG Fab'_2 fragments conjugated to HRP (Jackson ImmunoResearch; 109–036-088) were diluted 1:5,000 in PBS-T, added to the plates, and incubated again for 1 h at room temperature. Between each step, the plates were washed with PBS-T four times. Plates were finally developed using TMB substrate (Thermo Fisher Scientific; 34021); the reaction was stopped using 1 M sulfuric acid and the plates read at 450 nm. Sera were screened for binding at 1:500 dilution. Recombinant monoclonal antibodies were diluted to 10 µg/ml and serially diluted 1:3; the half effective concentration (EC_{50}) was determined by nonlinear regression analysis using Prism 8 (GraphPad). For cross-binding assays, recombinant antibodies were assayed at 1 µg/ml according to the protocol described above using the panel of flavivirus EDIII proteins. The anti-HIV monoclonal antibody 10–1074 was used

Downloaded from http://rupress.org/jem/article-pdf/218/5/e20210236/1803798/jem_20210236.pdf by guest on 18 January 2024

as isotype control (Mouquet et al., 2012). Antibodies with optical density >2.5 times isotype control signal were considered cross-reactive. The TBEV clinical tests (Table S1) were conducted using the EIA TBE Virus IgG (TBG096) and EIA TBE Virus IgM (TBM096) kits from TestLine Clinical Diagnostics.

Viruses and cells

The low-passage TBEV strain Hypr was provided by the Collection of Arboviruses, Institute of Parasitology, Biology Centre of the Czech Academy of Sciences, Ceske Budejovice, Czech Republic (http://www.arboviruscollection.cz/index.php?lang=en). The virus was originally isolated from the blood of a diseased 10-yr-old child in Brno, Czech Republic (formerly Czechoslovakia), in 1953. Prior to the use in in vitro and in vivo experiments, the virus was propagated in suckling mouse brains and/or BHK-21 cells.

PS (porcine kidney stable) cells (Kozuch and Mayer, 1975) were cultured at 37°C in Leibovitz (L-15) medium supplemented with 3% FBS, 100 U/ml penicillin, 100 µg/ml streptomycin, and 1% L-glutamine (Sigma-Aldrich).

Plaque assay

To determine virus titer, plaque assays were performed as previously described (De Madrid and Porterfield, 1969), with slight modifications (Pokorna Formanova et al., 2019). Briefly, 10-fold dilutions of virus plus a suspension of PS cells (1.3×10^5 cells per well) were added to 24-well tissue culture plates. After 4 h of incubation at 37°C with 0.5% CO_2, each well was overlaid with carboxymethylcellulose (1.5% in L-15 medium). After a 5-d incubation at 37°C and 0.5% CO_2, the cell monolayers were visualized using naphthalene black. Viral titers were expressed as PFU per milliliter.

Virus neutralization test

The virus neutralization test was performed as described previously (Širmarová et al., 2014), with several modifications. Briefly, monoclonal antibodies (T025, T028, T034, and T038) were diluted to 2.5 µg/ml in L-15 medium and then serially diluted 1:2 in 96-well plates. Diluted monoclonals were incubated with 50 PFU per well of TBEV-Hypr (sufficient to cause 90–95% cytolysis) for 90 min at 37°C. Thereafter, 5×10^4 PS cells were added per well. After 4-d incubation (37°C), the cytopathic effect was monitored microscopically, and cell viability was measured using the Cell Counting Kit-8 (Dojindo Molecular Technologies) according to the manufacturer's instructions. IC_{50} was calculated from two independent experiments done in octuplicates using GraphPad Prism (GraphPad Software; version 7.04).

Virus neutralization was also assayed using a fluorescence-based virus neutralization test. Monoclonal antibodies (T025, T028, T034, and T038; 10–1074 was used as an isotype control) were incubated with TBEV, and PS cells were infected as described above. The cells were incubated for 48 h at 37°C. The cell monolayers were fixed with cold acetone/methanol (1:1), blocked with 10% FBS, and incubated with mouse anti-flavivirus antibody (Sigma-Aldrich; 1:250 dilution, clone D1-4G2-4-15; catalog no. MAB10216). After washing, the cells were labeled with secondary goat anti-mouse antibody conjugated to FITC (Sigma-Aldrich; diluted 1:500, catalog no. AP181F) and counterstained with DAPI (diluted to 1 µg/ml) to visualize cell nuclei. The fluorescence signal was recorded with an Olympus IX71 epifluorescence microscope and processed by ImageJ software.

Statistical analyses

Data were analyzed using Mann–Whitney tests or ANOVA and Tukey's multiple comparison tests as specified and comparison of survival curves was analyzed by log-rank (Mantel–Cox) test, calculated in GraphPad Prism (version 8.4.3). P values < 0.05 were considered significant.

Crystallization, structure determination, and refinement

Complexes for crystallization were produced by mixing Fab and antigen at a 1:1 molar ratio and incubating at room temperature for 1–2 h. Crystals of T025 Fab–TBEV^{WE} EDIII-His-Avitag complex (space group $P2_1$; a = 55.5 Å, b = 66.7 Å, c = 91.2 Å, α = 90°, β = 94.6°, γ = 90°; one complex per asymmetric unit) were obtained by combining 0.2 µl crystallization complex with 0.2 µl of 0.1 M sodium citrate tribasic dihydrate, pH 5.0, 10% PEG 6000 in sitting drops at 22°C. Crystals of T025 Fab–TBEV^{FE} EDIII-His-Avitag complex (space group $P2_12_12$; a = 56.96 Å, b = 69.72 Å, c = 180.20 Å, α = 90°, β = 90°, γ = 90°; one complex per asymmetric unit) were obtained by combining 0.2 µl crystallization complex with 0.2 µl of 0.1 M sodium citrate tribasic dihydrate, pH 5.0, 10% PEG 6000 in sitting drops at 22°C. Crystals of T025 Fab–TBEV^{Si} EDIII complex (space group $P2_1$; a = 55.4 Å, b = 67.2 Å, c = 91.2 Å, α = 90°, β = 94.8°, γ = 90°; one complex per asymmetric unit) were obtained by combining 0.2 µl crystallization complex with 0.2 µl of 5% (±)-2-methyl-2,4-pentanediol, 0.1 M Hepes, pH 7.5, 10% PEG 10,000 in sitting drops at 22°C. Crystals were cryoprotected with 25% glycerol before being cryopreserved in liquid nitrogen.

X-ray diffraction data were collected at Stanford Synchrotron Radiation Lightsource Beamline 12–2 using a Dectris Pilatus 6M detector. The data were integrated using Mosflm (Battye et al., 2011) and scaled using CCP4 (Winn et al., 2011). The T025-TBEV^{WE} EDIII complex structure was solved by molecular replacement using the V_HV_L domains from PDB accession no. 2GHW, the C_HC_L domains from PDB accession no. 4OGX, and TBEV EDIII from PDB accession no. 6J5F as search models in PHASER (McCoy et al., 2007). The model was refined to 2.24 Å resolution using an iterative approach involving refinement in Phenix (Adams et al., 2010) and manual rebuilding into a simulated annealed composite omit map using Coot (Emsley and Cowtan, 2004). Residues that were disordered and not included in the model were HC residues 131–132, 214–219 and the 6XHis tag; residue 214 of the LC; and residues 299–302, 397, and the 6XHis tag and Avi tag of the TBEV^{WE} EDIII domain. The T025-TBEV^{FE} EDIII and T025-TBEV^{Si} EDIII complex structures were solved similarly using the partially refined T025-TBEV^{WE} EDIII structure as the molecular replacement model. The T025-TBEV^{FE} EDIII model was refined to 2.35 Å resolution, and the T025-TBEV^{Si} EDIII model was refined to 1.86 Å resolution using the iterative approach described for T025-TBEV^{WE} EDIII. The Kabat numbering scheme was used for Fab numbering. Structures were superimposed, RMSDs were calculated, and figures

Downloaded from http://rupress.org/jem/article-pdf/218/5/e20210236/1803798/jem_20210236.pdf by guest on 18 January 2024

were generated using PyMOL. Buried surface areas and hydrogen bonds were determined using PDBePISA (Krissinel and Henrick, 2007). Fab-antigen contact residues were identified as residues in which any atom is within 4 Å of an atom on the other protein. The distance and geometry criteria used for assigning hydrogen bonds were a distance of <4.0 Å and a hydrogen bond angle of 90–270°. The maximum distance allowed for a van der Waals interaction was 4.0 Å.

Animal ethics statement

The research complied with all relevant European Union guidelines for work with animals and was in accordance with Czech national law guidelines on the use of experimental animals and protection of animals against cruelty (Animal Welfare Act No. 246/1992 Coll.). The protocol was approved by the Committee on the Ethics of Animal Experimentation of the Institute of Parasitology and the Departmental Expert Committee for the Approval of Projects of Experiments on Animals of the Czech Academy of Sciences (permit no. 4253/2019).

Mice and virus inoculation

Specific pathogen–free BALB/c mice were obtained from ENVIGO RMS. Sterilized pellet diet and water were supplied ad libitum. In all experiments, female mice aged 6–8 wk were used. Mice were housed in individually ventilated plastic cages (Techniplast) with wood-chip bedding, with a constant temperature of 22°C, a relative humidity of 65%, and under a 12-h light/dark cycle. Three mice per group were used in experiments. Mice were inoculated i.p. 1 d before or 1, 3, or 5 d after infection with monoclonal antibodies T025 or 10–1074 in 200 µl PBS and infected subcutaneously with 100 PFU TBEV-Hypr (propagated eight times in suckling mouse brains). Mice were monitored for symptoms and survival over time and euthanized when reaching a humane endpoint.

Online supplemental material

Fig. S1 shows correlations between clinical or demographic data, donor serum RVP neutralization or EDIII binding profiles, and RVP neutralization curves for vaccinee serum. Fig. S2 includes the single-cell sorting strategy, somatic hypermutations, and CDR3 length analysis for individual donors and all donors grouped together, as well as hydrophobicity GRAVY scores. Fig. S3 shows VH, VK, and VL gene frequencies; CDR3 sequence logos; and examples of antibody genes and CDR3 sequences that are similar across donors. Fig. S4 includes antibody binding to $TBEV^{FE}$ and $TBEV^{Si}$ by ELISA, screening results for antibody binding and neutralization of related tick-borne flaviviruses, and neutralization curves for selected antibodies against related tick-borne flaviviruses. Fig. S5 shows overlay of T025 crystal structures with the three TBEV-lineage EDIIIs, the amino acid alignment of three TBEV-lineage EDIIIs, and contact residues between T025 and TBEV EDIII. Table S1 contains clinical and demographic data for infected and vaccinated donors. Table S2 includes all antibody sequences obtained from sorted donor samples. Table S3 includes the sequences of antibodies that are similar across donors. Table S4 contains the sequences of the monoclonal antibodies that were cloned and recombinantly expressed. Table S5 shows EC_{50} and IC_{50} values for all antibodies tested. Table S6 contains data collection and refinement statistics for the crystal structures.

Acknowledgments

We especially thank the study participants of České Budějovice and Brno who agreed to take part in this study, as well as the staff of the Hospital České Budějovice for their assistance with the clinical protocols, and all members of the Nussenzweig laboratory for discussions. We are grateful to Mary Ellen Castillo and Andrea Jurado for facilitating work with reporter viruses and Zoran Jankovic and Masa Jankovic for laboratory support. We thank Pauline Hoffman, Jost Vielmetter, and the Caltech Beckman Institute Protein Expression Center for expression and purification of Fabs and Harry B. Gristick and Christopher O. Barnes for assistance with crystallographic methods and helpful discussions. We also thank Jens Kaiser from the Molecular Observatory at the Beckman Institute at the California Institute of Technology and the staff at Beamline 12–2, Stanford Synchrotron Radiation Lightsource for their assistance with crystallographic data collection and processing.

This work was supported by National Institutes of Health pilot award U19AI111825 and Swiss National Science Foundation grant IRB startup funds (to D.F. Robbiani) and grants R01AI037526, UM1AI100663, U19AI111825, and UL1TR001866 (to M.C. Nussenzweig), P01AI138938 (to M.C. Nussenzweig, P.J. Bjorkman, and C.M. Rice), R01AI124690 (to C.M. Rice), and U19AI057229 (CCHI Opportunity Fund Project to C.M. Rice and M.R. MacDonald). This work was also supported by Czech Science Foundation grants 20-14325S and 20-30500S (to D. Růžek and M. Palus), Czech Academy of Sciences grant MSM200962002 (to M. Palus), and Ministry of Health of the Czech Republic grant NV19-05-00457 (to D. Růžek). Operations at the Stanford Synchrotron Radiation Lightsource are supported by the U.S. Department of Energy and the National Institutes of Health. M.C. Nussenzweig is an investigator of the Howard Hughes Medical Institute.

Author contributions: M. Agudelo conducted experiments, supervised and designed experiments, interpreted data, and wrote the paper. M. Palus, J. Salát, and P. Svoboda designed and conducted experiments with viruses, interpreted data, edited the paper, and together with J. Elsterová and V. Hönig coordinated and assisted in blood collection. A. Chrdle and D. Teislerová were responsible for the recruitment of the participants and blood collection. J.R. Keeffe solved and analyzed crystal structures with Y.E. Lee, and wrote structural portions of the paper with P.J. Bjorkman. F. Bianchini, A. Gazumyan, M. Cipolla, T. Kapoor, A. Peace, F. Guidetti, and K-H. Yao conducted experiments. T. Oliveira and A.P. West, Jr. performed statistical and computational analysis. C.M. Rice and M.R. MacDonald supervised and interpreted experimental results. D. Růžek coordinated clinical cohorts, supervised and designed experiments with viruses, interpreted data, and edited the paper. D.F. Robbiani and M.C. Nussenzweig supervised, designed, and interpreted experiments and wrote the paper.

Downloaded from http://rupress.org/jem/article-pdf/218/5/e20210236/1803798/jem_20210236.pdf by guest on 18 January 2024

Disclosures: M. Agudelo, D.F. Robbiani, and M.C. Nussenzweig reported a patent to Broadly Neutralizing Antibodies to Tick-Borne Encephalitis and Related Viruses (US 63/118,461) pending. M.C. Nussenzweig reported personal fees from Celldex outside the submitted work. Additionally, M.C. Nussenzweig is a Frontier Bioscience SAB member. No other disclosures were reported.

Submitted: 28 January 2021
Revised: 17 February 2021
Accepted: 19 February 2021

References

Adams, P.D., P.V. Afonine, G. Bunkóczi, V.B. Chen, I.W. Davis, N. Echols, J.J. Headd, L.W. Hung, G.J. Kapral, R.W. Grosse-Kunstleve, et al. 2010. PHENIX: a comprehensive Python-based system for macromolecular structure solution. *Acta Crystallogr. D Biol. Crystallogr.* 66:213–221. https://doi.org/10.1107/S0907444909052925

Albinsson, B., S. Vene, L. Rombo, J. Blomberg, Å. Lundkvist, and B. Rönnberg. 2018. Distinction between serological responses following tick-borne encephalitis virus (TBEV) infection vs vaccination, Sweden 2017. *Euro Surveill.* 23:17–00838. https://doi.org/10.2807/1560-7917.ES.2018.23.3.17-00838

Arras, C., R. Fescharek, and J.P. Gregersen. 1996. Do specific hyper-immunoglobulins aggravate clinical course of tick-borne encephalitis? *Lancet.* 347:1331. https://doi.org/10.1016/S0140-6736(96)90977-0

Battye, T.G., L. Kontogiannis, O. Johnson, H.R. Powell, and A.G. Leslie. 2011. iMOSFLM: a new graphical interface for diffraction-image processing with MOSFLM. *Acta Crystallogr. D Biol. Crystallogr.* 67:271–281. https://doi.org/10.1107/S0907444910048675

Baykov, I.K., A.L. Matveev, O.V. Stronin, A.B. Ryzhikov, L.E. Matveev, M.F. Kasakin, V.A. Richter, and N.V. Tikunova. 2014. A protective chimeric antibody to tick-borne encephalitis virus. *Vaccine.* 32:3589–3594. https://doi.org/10.1016/j.vaccine.2014.05.012

Beasley, D.W., and A.D. Barrett. 2002. Identification of neutralizing epitopes within structural domain III of the West Nile virus envelope protein. *J. Virol.* 76:13097–13100. https://doi.org/10.1128/JVI.76.24.13097-13100.2002

Beauté, J., G. Spiteri, E. Warns-Petit, and H. Zeller. 2018. Tick-borne encephalitis in Europe, 2012 to 2016. *Euro Surveill.* 23:1800201. https://doi.org/10.2807/1560-7917.ES.2018.23.45.1800201

Beltramello, M., K.L. Williams, C.P. Simmons, A. Macagno, L. Simonelli, N.T. Quyen, S. Sukupolvi-Petty, E. Navarro-Sanchez, P.R. Young, A.M. de Silva, et al. 2010. The human immune response to Dengue virus is dominated by highly cross-reactive antibodies endowed with neutralizing and enhancing activity. *Cell Host Microbe.* 8:271–283. https://doi.org/10.1016/j.chom.2010.08.007

Bogovic, P., and F. Strle. 2015. Tick-borne encephalitis: A review of epidemiology, clinical characteristics, and management. *World J. Clin. Cases.* 3:430–441. https://doi.org/10.12998/wjcc.v3.i5.430

Bogovič, P., S. Lotrič-Furlan, T. Avšič-Županc, L. Lusa, and F. Strle. 2018a. Factors associated with severity of tick-borne encephalitis: A prospective observational study. *Travel Med. Infect. Dis.* 26:25–31. https://doi.org/10.1016/j.tmaid.2018.10.003

Bogovič, P., D. Stupica, T. Rojko, S. Lotrič-Furlan, T. Avšič-Županc, A. Kastrin, L. Lusa, and F. Strle. 2018b. The long-term outcome of tick-borne encephalitis in Central Europe. *Ticks Tick Borne Dis.* 9:369–378. https://doi.org/10.1016/j.ttbdis.2017.12.001

Briney, B., A. Inderbitzin, C. Joyce, and D.R. Burton. 2019. Commonality despite exceptional diversity in the baseline human antibody repertoire. *Nature.* 566:393–397. https://doi.org/10.1038/s41586-019-0879-y

Caini, S., K. Szomor, E. Ferenczi, A. Szekelyne Gaspar, A. Csohan, K. Krisztalovics, Z. Molnar, and J. Horvath. 2012. Tick-borne encephalitis transmitted by unpasteurised cow milk in western Hungary, September to October 2011. *Euro Surveill.* 17:17.

Calisher, C.H., N. Karabatsos, J.M. Dalrymple, R.E. Shope, J.S. Porterfield, E.G. Westaway, and W.E. Brandt. 1989. Antigenic relationships between flaviviruses as determined by cross-neutralization tests with polyclonal antisera. *J. Gen. Virol.* 70:37–43. https://doi.org/10.1099/0022-1317-70-1-37

Chen, F., N. Tzarum, I.A. Wilson, and M. Law. 2019. V_H1-69 antiviral broadly neutralizing antibodies: genetics, structures, and relevance to rational vaccine design. *Curr. Opin. Virol.* 34:149–159. https://doi.org/10.1016/j.coviro.2019.02.004

Cisak, E., A. Wójcik-Fatla, V. Zając, J. Sroka, A. Buczek, and J. Dutkiewicz. 2010. Prevalence of tick-borne encephalitis virus (TBEV) in samples of raw milk taken randomly from cows, goats and sheep in eastern Poland. *Ann. Agric. Environ. Med.* 17:283–286.

Crill, W.D., and J.T. Roehrig. 2001. Monoclonal antibodies that bind to domain III of dengue virus E glycoprotein are the most efficient blockers of virus adsorption to Vero cells. *J. Virol.* 75:7769–7773. https://doi.org/10.1128/JVI.75.16.7769-7773.2001

Crooks, G.E., G. Hon, J.M. Chandonia, and S.E. Brenner. 2004. WebLogo: a sequence logo generator. *Genome Res.* 14:1188–1190. https://doi.org/10.1101/gr.849004

De Madrid, A.T., and J.S. Porterfield. 1969. A simple micro-culture method for the study of group B arboviruses. *Bull. World Health Organ.* 40:113–121.

DeWitt, W.S., P. Lindau, T.M. Snyder, A.M. Sherwood, M. Vignali, C.S. Carlson, P.D. Greenberg, N. Duerkopp, R.O. Emerson, and H.S. Robins. 2016. A Public Database of Memory and Naive B-Cell Receptor Sequences. *PLoS One.* 11:e0160853. https://doi.org/10.1371/journal.pone.0160853

Dobler, G., K. Kaier, P. Hehn, M.M. Böhmer, T.M. Kreusch, and J.P. Borde. 2020. Tick-borne encephalitis virus vaccination breakthrough infections in Germany: a retrospective analysis from 2001 to 2018. *Clin. Microbiol. Infect.* 26:1090.e7–1090.e13. https://doi.org/10.1016/j.cmi.2019.12.001

Donoso-Mantke, O., L.S. Karan, and D. Růžek. 2011. Tick-Borne Encephalitis Virus: A General Overview. *In* Flavivirus Encephalitis. D. Růžek, editor. InTech, Rijeka, Croatia. pp. 133–156. https://doi.org/10.5772/21912

Edeling, M.A., S.K. Austin, B. Shrestha, K.A. Dowd, S. Mukherjee, C.A. Nelson, S. Johnson, M.N. Mabila, E.A. Christian, J. Rucker, et al. 2014. Potent dengue virus neutralization by a therapeutic antibody with low monovalent affinity requires bivalent engagement. *PLoS Pathog.* 10:e1004072. https://doi.org/10.1371/journal.ppat.1004072

Emsley, P., and K. Cowtan. 2004. Coot: model-building tools for molecular graphics. *Acta Crystallogr. D Biol. Crystallogr.* 60:2126–2132. https://doi.org/10.1107/S0907444904019158

Füzik, T., P. Formanová, D. Růžek, K. Yoshii, M. Niedrig, and P. Plevka. 2018. Structure of tick-borne encephalitis virus and its neutralization by a monoclonal antibody. *Nat. Commun.* 9:436. https://doi.org/10.1038/s41467-018-02882-0

Girl, P., M. Bestehorn-Willmann, S. Zange, J.P. Borde, G. Dobler, and H. von Buttlar. 2020. Tick-Borne Encephalitis Virus Nonstructural Protein 1 IgG Enzyme-Linked Immunosorbent Assay for Differentiating Infection versus Vaccination Antibody Responses. *J. Clin. Microbiol.* 58:e01783-19. https://doi.org/10.1128/JCM.01783-19

Gould, E.A., and T. Solomon. 2008. Pathogenic flaviviruses. *Lancet.* 371:500–509. https://doi.org/10.1016/S0140-6736(08)60238-X

Gupta, N.T., J.A. Vander Heiden, M. Uduman, D. Gadala-Maria, G. Yaari, and S.H. Kleinstein. 2015. Change-O: a toolkit for analyzing large-scale B cell immunoglobulin repertoire sequencing data. *Bioinformatics.* 31:3356–3358. https://doi.org/10.1093/bioinformatics/btv359

Guy, H.R. 1985. Amino acid side-chain partition energies and distribution of residues in soluble proteins. *Biophys. J.* 47:61–70. https://doi.org/10.1016/S0006-3495(85)83877-7

Halstead, S.B. 2014. Dengue Antibody-Dependent Enhancement: Knowns and Unknowns. *Microbiol. Spectr.* 2:2.

Holzmann, H. 2003. Diagnosis of tick-borne encephalitis. *Vaccine.* 21(Suppl 1):S36–S40. https://doi.org/10.1016/S0264-410X(02)00819-8

Holzmann, H., S.W. Aberle, K. Stiasny, P. Werner, A. Mischak, B. Zainer, M. Netzer, S. Koppi, E. Bechter, and F.X. Heinz. 2009. Tick-borne encephalitis from eating goat cheese in a mountain region of Austria. *Emerg. Infect. Dis.* 15:1671–1673. https://doi.org/10.3201/eid1510.090743

Kaiser, R. 2008. Tick-borne encephalitis. *Infect. Dis. Clin. North Am.* 22:561–575: x. https://doi.org/10.1016/j.idc.2008.03.013

Keeffe, J.R., K.K.A. Van Rompay, P.C. Olsen, Q. Wang, A. Gazumyan, S.A. Azzopardi, D. Schaefer-Babajew, Y.E. Lee, J.B. Stuart, A. Singapuri, et al. 2018. A Combination of Two Human Monoclonal Antibodies Prevents Zika Virus Escape Mutations in Non-human Primates. *Cell Rep.* 25:1385–1394.e7. https://doi.org/10.1016/j.celrep.2018.10.031

Kenney, J.L., M. Anishchenko, M. Hermance, H. Romo, C.I. Chen, S. Thangamani, and A.C. Brault. 2018. Generation of a Lineage II Powassan

Downloaded from http://rupress.org/jem/article-pdf/218/5/e20210236/1803798/jem_20210236.pdf by guest on 18 January 2024

Virus (Deer Tick Virus) cDNA Clone: Assessment of Flaviviral Genetic Determinants of Tick and Mosquito Vector Competence. *Vector Borne Zoonotic Dis.* 18:371–381. https://doi.org/10.1089/vbz.2017.2224

Klein, F., L. Nogueira, Y. Nishimura, G. Phad, A.P. West Jr., A. Halper-Stromberg, J.A. Horwitz, A. Gazumyan, C. Liu, T.R. Eisenreich, et al. 2014. Enhanced HIV-1 immunotherapy by commonly arising antibodies that target virus escape variants. *J. Exp. Med.* 211:2361–2372. https://doi.org/10.1084/jem.20141050

Kluger, G., A. Schöttler, K. Waldvogel, D. Nadal, W. Hinrichs, G.F. Wündisch, and M.C. Laub. 1995. Tickborne encephalitis despite specific immunoglobulin prophylaxis. *Lancet.* 346:1502. https://doi.org/10.1016/S0140-6736(95)92527-9

Kollaritsch, H., V. Chmelík, I. Dontsenko, A. Grzeszczuk, M. Kondrusik, V. Usonis, and A. Lakos. 2011. The current perspective on tick-borne encephalitis awareness and prevention in six Central and Eastern European countries: report from a meeting of experts convened to discuss TBE in their region. *Vaccine.* 29:4556–4564. https://doi.org/10.1016/j.vaccine.2011.04.061

Kozuch, O., and V. Mayer. 1975. Pig kidney epithelial (PS) cells: a perfect tool for the study of flaviviruses and some other arboviruses. *Acta Virol.* 19:498.

Kreil, T.R., E. Maier, S. Fraiss, and M.M. Eibl. 1998. Neutralizing antibodies protect against lethal flavivirus challenge but allow for the development of active humoral immunity to a nonstructural virus protein. *J. Virol.* 72:3076–3081. https://doi.org/10.1128/JVI.72.4.3076-3081.1998

Krissinel, E., and K. Henrick. 2007. Inference of macromolecular assemblies from crystalline state. *J. Mol. Biol.* 372:774–797. https://doi.org/10.1016/j.jmb.2007.05.022

Kuno, G., G.-J.J. Chang, K.R. Tsuchiya, N. Karabatsos, and C.B. Cropp. 1998. Phylogeny of the genus Flavivirus. *J. Virol.* 72:73–83. https://doi.org/10.1128/JVI.72.1.73-83.1998

Kyte, J., and R.F. Doolittle. 1982. A simple method for displaying the hydropathic character of a protein. *J. Mol. Biol.* 157:105–132. https://doi.org/10.1016/0022-2836(82)90515-0

Lai, C.Y., W.Y. Tsai, S.R. Lin, C.L. Kao, H.P. Hu, C.C. King, H.C. Wu, G.J. Chang, and W.K. Wang. 2008. Antibodies to envelope glycoprotein of dengue virus during the natural course of infection are predominantly cross-reactive and recognize epitopes containing highly conserved residues at the fusion loop of domain II. *J. Virol.* 82:6631–6643. https://doi.org/10.1128/JVI.00316-08

LaSala, P.R., and M. Holbrook. 2010. Tick-borne flaviviruses. *Clin. Lab. Med.* 30:221–235. https://doi.org/10.1016/j.cll.2010.01.002

Levanov, L.N., L.E. Matveev, E.P. Goncharova, L.R. Lebedev, A.B. Ryzhikov, T.E. Yun, T.A. Batanova, A.N. Shvalov, I.K. Baykov, L.N. Shingarova, et al. 2010. Chimeric antibodies against tick-borne encephalitis virus. *Vaccine.* 28:5265–5271. https://doi.org/10.1016/j.vaccine.2010.05.060

Loew-Baselli, A., E.-M. Poellabauer, B.G. Pavlova, S. Fritsch, M. Koska, R. Bobrovsky, R. Konior, and H.J. Ehrlich. 2009. Seropersistence of tick-borne encephalitis antibodies, safety and booster response to FSME-IMMUN 0.5 ml in adults aged 18-67 years. *Hum. Vaccin.* 5:551–556. https://doi.org/10.4161/hv.5.8.8571

Lotrič-Furlan, S., P. Bogovič, T. Avšič-Županc, M. Jelovšek, L. Lusa, and F. Strle. 2017. Tick-borne encephalitis in patients vaccinated against this disease. *J. Intern. Med.* 282:142–155. https://doi.org/10.1111/joim.12625

Maikova, G.B., L.L. Chernokhaeva, Y.V. Rogova, L.I. Kozlovskaya, I.S. Kholodilov, V.V. Romanenko, M.S. Esyunina, A.A. Ankudinova, A.S. Kilyachina, M.F. Vorovitch, and G.G. Karganova. 2019. Ability of inactivated vaccines based on far-eastern tick-borne encephalitis virus strains to induce humoral immune response in originally seropositive and seronegative recipients. *J. Med. Virol.* 91:190–200. https://doi.org/10.1002/jmv.25316

Mansfield, K.L., D.L. Horton, N. Johnson, L. Li, A.D.T. Barrett, D.J. Smith, S.E. Galbraith, T. Solomon, and A.R. Fooks. 2011. Flavivirus-induced antibody cross-reactivity. *J. Gen. Virol.* 92:2821–2829. https://doi.org/10.1099/vir.0.031641-0

Matveev, A., L. Matveev, O. Stronin, I. Baykov, L. Emeljanova, Y. Khlusevich, and N. Tikunova. 2020. Characterization of neutralizing monoclonal antibody against tick-borne encephalitis virus in vivo. *Vaccine.* 38:4309–4315. https://doi.org/10.1016/j.vaccine.2020.04.051

Matveeva, V.A., R.V. Popova, E.A. Kvetkova, L.O. Chernicina, V.I. Zlobin, N.M. Puchovskaya, and O.V. Morozova. 1995. Antibodies against tick-borne encephalitis virus (TBEV) non-structural and structural proteins in human sera and spinal fluid. *Immunol. Lett.* 46:1–4. https://doi.org/10.1016/0165-2478(95)00021-V

McAuley, A.J., B. Sawatsky, T. Ksiazek, M. Torres, M. Korva, S. Lotrič-Furlan, T. Avšič-Županc, V. von Messling, M.R. Holbrook, A.N. Freiberg, et al. 2017. Cross-neutralisation of viruses of the tick-borne encephalitis complex following tick-borne encephalitis vaccination and/or infection. *NPJ Vaccines.* 2:5. https://doi.org/10.1038/s41541-017-0009-5

McCoy, A.J., R.W. Grosse-Kunstleve, P.D. Adams, M.D. Winn, L.C. Storoni, and R.J. Read. 2007. Phaser crystallographic software. *J. Appl. Cryst.* 40:658–674. https://doi.org/10.1107/S0021889807021206

Morens, D.M., and A.S. Fauci. 2020. Emerging Pandemic Diseases: How We Got to COVID-19. *Cell.* 182:1077–1092. https://doi.org/10.1016/j.cell.2020.08.021

Mouquet, H., L. Scharf, Z. Euler, Y. Liu, C. Eden, J.F. Scheid, A. Halper-Stromberg, P.N. Gnanapragasam, D.I. Spencer, M.S. Seaman, et al. 2012. Complex-type N-glycan recognition by potent broadly neutralizing HIV antibodies. *Proc. Natl. Acad. Sci. USA.* 109:E3268–E3277. https://doi.org/10.1073/pnas.1217207109

Nybakken, G.E., T. Oliphant, S. Johnson, S. Burke, M.S. Diamond, and D.H. Fremont. 2005. Structural basis of West Nile virus neutralization by a therapeutic antibody. *Nature.* 437:764–769. https://doi.org/10.1038/nature03956

Pen'evskaia, N.A., and N.V. Rudakov. 2010. [Efficiency of use of immunoglobulin preparations for the postexposure prevention of tick-borne encephalitis in Russia (a review of semi-centennial experience)]. *Med. Parazitol. (Mosk.).* 1:53–59.

Phillpotts, R.J., J.R. Stephenson, and J.S. Porterfield. 1985. Antibody-dependent enhancement of tick-borne encephalitis virus infectivity. *J. Gen. Virol.* 66:1831–1837. https://doi.org/10.1099/0022-1317-66-8-1831

Pierson, T.C., M.D. Sánchez, B.A. Puffer, A.A. Ahmed, B.J. Geiss, L.E. Valentine, L.A. Altamura, M.S. Diamond, and R.W. Doms. 2006. A rapid and quantitative assay for measuring antibody-mediated neutralization of West Nile virus infection. *Virology.* 346:53–65. https://doi.org/10.1016/j.virol.2005.10.030

Pierson, T.C., D.H. Fremont, R.J. Kuhn, and M.S. Diamond. 2008. Structural insights into the mechanisms of antibody-mediated neutralization of flavivirus infection: implications for vaccine development. *Cell Host Microbe.* 4:229–238. https://doi.org/10.1016/j.chom.2008.08.004

Pokorna Formanova, P., M. Palus, J. Salat, V. Hönig, M. Stefanik, P. Svoboda, and D. Ruzek. 2019. Changes in cytokine and chemokine profiles in mouse serum and brain, and in human neural cells, upon tick-borne encephalitis virus infection. *J. Neuroinflammation.* 16:205. https://doi.org/10.1186/s12974-019-1596-z

Pulkkinen, L.I.A., S.J. Butcher, and M. Anastasina. 2018. Tick-Borne Encephalitis Virus: A Structural View. *Viruses.* 10:350. https://doi.org/10.3390/v10070350

Rabel, P.O., C.B. Planitzer, M.R. Farcet, and T.R. Kreil. 2012. Tick-borne encephalitis virus-neutralizing antibodies in different immunoglobulin preparations. *Clin. Vaccine Immunol.* 19:623–625. https://doi.org/10.1128/CVI.05705-11

Ramaraj, T., T. Angel, E.A. Dratz, A.J. Jesaitis, and B. Mumey. 2012. Antigen-antibody interface properties: composition, residue interactions, and features of 53 non-redundant structures. *Biochim. Biophys. Acta.* 1824:520–532. https://doi.org/10.1016/j.bbapap.2011.12.007

Remoli, M.E., A. Marchi, C. Fortuna, E. Benedetti, G. Minelli, C. Fiorentini, R. Mel, G. Venturi, and M.G. Ciufolini. 2015. Anti-tick-borne encephalitis (TBE) virus neutralizing antibodies dynamics in natural infections versus vaccination. *Pathog. Dis.* 73:1–3. https://doi.org/10.1093/femspd/ftu002

Renner, M., A. Flanagan, W. Dejnirattisai, C. Puttikhunt, W. Kasinrerk, P. Supasa, W. Wongwiwat, K. Chawansuntati, T. Duangchinda, A. Cowper, et al. 2018. Characterization of a potent and highly unusual minimally enhancing antibody directed against dengue virus. *Nat. Immunol.* 19:1248–1256. https://doi.org/10.1038/s41590-018-0227-7

Rey, F.A., F.X. Heinz, C. Mandl, C. Kunz, and S.C. Harrison. 1995. The envelope glycoprotein from tick-borne encephalitis virus at 2 A resolution. *Nature.* 375:291–298. https://doi.org/10.1038/375291a0

Robbiani, D.F., L. Bozzacco, J.R. Keeffe, R. Khouri, P.C. Olsen, A. Gazumyan, D. Schaefer-Babajew, S. Avila-Rios, L. Nogueira, R. Patel, et al. 2017. Recurrent Potent Human Neutralizing Antibodies to Zika Virus in Brazil and Mexico. *Cell.* 169:597–609.e11. https://doi.org/10.1016/j.cell.2017.04.024

Robbiani, D.F., C. Gaebler, F. Muecksch, J.C.C. Lorenzi, Z. Wang, A. Cho, M. Agudelo, C.O. Barnes, A. Gazumyan, S. Finkin, et al. 2020. Convergent antibody responses to SARS-CoV-2 in convalescent individuals. *Nature.* 584:437–442. https://doi.org/10.1038/s41586-020-2456-9

Rock, E.P., P.R. Sibbald, M.M. Davis, and Y.H. Chien. 1994. CDR3 length in antigen-specific immune receptors. *J. Exp. Med.* 179:323–328. https://doi.org/10.1084/jem.179.1.323

Downloaded from http://rupress.org/jem/article-pdf/218/5/e20210236/1803798/jem_20210236.pdf by guest on 18 January 2024

Roehrig, J.T. 2003. Antigenic structure of flavivirus proteins. *Adv. Virus Res.* 59:141–175. https://doi.org/10.1016/S0065-3527(03)59005-4

Rubelt, F., V. Sievert, F. Knaust, C. Diener, T.S. Lim, K. Skriner, E. Klipp, R. Reinhardt, H. Lehrach, and Z. Konthur. 2012. Onset of immune senescence defined by unbiased pyrosequencing of human immunoglobulin mRNA repertoires. *PLoS One.* 7:e49774. https://doi.org/10.1371/journal.pone.0049774

Russian Ministry of Health. 2008. Sanitary and Epidemiological Rules SP 3.1.3.2352-08. Russian Ministry of Health, Moscow.

Ruzek, D., T. Avšič Županc, J. Borde, A. Chrdle, L. Eyer, G. Karganova, I. Kholodilov, N. Knap, L. Kozlovskaya, A. Matveev, et al. 2019. Tick-borne encephalitis in Europe and Russia: Review of pathogenesis, clinical features, therapy, and vaccines. *Antiviral Res.* 164:23–51. https://doi.org/10.1016/j.antiviral.2019.01.014

Sapparapu, G., E. Fernandez, N. Kose, J.M. Bin Cao, J.M. Fox, R.G. Bombardi, H. Zhao, C.A. Nelson, A.L. Bryan, T. Barnes, et al. 2016. Neutralizing human antibodies prevent Zika virus replication and fetal disease in mice. *Nature.* 540:443–447. https://doi.org/10.1038/nature20564

Scheid, J.F., H. Mouquet, B. Ueberheide, R. Diskin, F. Klein, T.Y. Oliveira, J. Pietzsch, D. Fenyo, A. Abadir, K. Velinzon, et al. 2011. Sequence and structural convergence of broad and potent HIV antibodies that mimic CD4 binding. *Science.* 333:1633–1637. https://doi.org/10.1126/science.1207227

Screaton, G., J. Mongkolsapaya, S. Yacoub, and C. Roberts. 2015. New insights into the immunopathology and control of dengue virus infection. *Nat. Rev. Immunol.* 15:745–759. https://doi.org/10.1038/nri3916

Širmarová, J., L. Tichá, M. Golovchenko, J. Salát, L. Grubhoffer, N. Rudenko, N. Nowotny, and D. Růžek. 2014. Seroprevalence of Borrelia burgdorferi sensu lato and tick-borne encephalitis virus in zoo animal species in the Czech Republic. *Ticks Tick Borne Dis.* 5:523–527. https://doi.org/10.1016/j.ttbdis.2014.03.008

Smura, T., E. Tonteri, A. Jääskeläinen, G. von Troil, S. Kuivanen, O. Huitu, L. Kareinen, J. Uusitalo, R. Uusitalo, T. Hannila-Handelberg, et al. 2019. Recent establishment of tick-borne encephalitis foci with distinct viral lineages in the Helsinki area, Finland. *Emerg. Microbes Infect.* 8:675–683. https://doi.org/10.1080/22221751.2019.1612279

Stettler, K., M. Beltramello, D.A. Espinosa, V. Graham, A. Cassotta, S. Bianchi, F. Vanzetta, A. Minola, S. Jaconi, F. Mele, et al. 2016. Specificity, cross-reactivity, and function of antibodies elicited by Zika virus infection. *Science.* 353:823–826. https://doi.org/10.1126/science.aaf8505

Sun, H., Q. Chen, and H. Lai. 2017. Development of Antibody Therapeutics against Flaviviruses. *Int. J. Mol. Sci.* 19:19.

Süss, J., C. Klaus, R. Diller, C. Schrader, N. Wohanka, and U. Abel. 2006. TBE incidence versus virus prevalence and increased prevalence of the TBE virus in Ixodes ricinus removed from humans. *Int. J. Med. Microbiol.* 296(Suppl 40):63–68. https://doi.org/10.1016/j.ijmm.2005.12.005

Thompson, B.S., B. Moesker, J.M. Smit, J. Wilschut, M.S. Diamond, and D.H. Fremont. 2009. A therapeutic antibody against west nile virus neutralizes infection by blocking fusion within endosomes. *PLoS Pathog.* 5:e1000453. https://doi.org/10.1371/journal.ppat.1000453

Tiller, T., M. Tsuiji, S. Yurasov, K. Velinzon, M.C. Nussenzweig, and H. Wardemann. 2007. Autoreactivity in human IgG+ memory B cells. *Immunity.* 26:205–213. https://doi.org/10.1016/j.immuni.2007.01.009

Vorovitch, M.F., G.B. Maikova, L.L. Chernokhaeva, V.V. Romanenko, G.G. Karganova, and A.A. Ishmukhametov. 2019. Comparison of the immunogenicity and safety of two pediatric TBE vaccines based on the Far Eastern and European virus subtypes. *Adv. Virol.* 2019:5323428. https://doi.org/10.1155/2019/5323428

Wahala, W.M., A.A. Kraus, L.B. Haymore, M.A. Accavitti-Loper, and A.M. de Silva. 2009. Dengue virus neutralization by human immune sera: role of envelope protein domain III-reactive antibody. *Virology.* 392:103–113. https://doi.org/10.1016/j.virol.2009.06.037

Waldvogel, K., W. Bossart, T. Huisman, E. Boltshauser, and D. Nadal. 1996. Severe tick-borne encephalitis following passive immunization. *Eur. J. Pediatr.* 155:775–779. https://doi.org/10.1007/BF02002905

Wang, Q., E. Michailidis, Y. Yu, Z. Wang, A.M. Hurley, D.A. Oren, C.T. Mayer, A. Gazumyan, Z. Liu, Y. Zhou, et al. 2020. A Combination of Human Broadly Neutralizing Antibodies against Hepatitis B Virus HBsAg with Distinct Epitopes Suppresses Escape Mutations. *Cell Host Microbe.* 28:335–349.e6. https://doi.org/10.1016/j.chom.2020.05.010

West, A.P. Jr., R. Diskin, M.C. Nussenzweig, and P.J. Bjorkman. 2012. Structural basis for germ-line gene usage of a potent class of antibodies targeting the CD4-binding site of HIV-1 gp120. *Proc. Natl. Acad. Sci. USA.* 109:E2083–E2090. https://doi.org/10.1073/pnas.1208984109

West, A.P. Jr., L. Scharf, J. Horwitz, F. Klein, M.C. Nussenzweig, and P.J. Bjorkman. 2013. Computational analysis of anti-HIV-1 antibody neutralization panel data to identify potential functional epitope residues. *Proc. Natl. Acad. Sci. USA.* 110:10598–10603. https://doi.org/10.1073/pnas.1309215110

Winn, M.D., C.C. Ballard, K.D. Cowtan, E.J. Dodson, P. Emsley, P.R. Evans, R.M. Keegan, E.B. Krissinel, A.G. Leslie, A. McCoy, et al. 2011. Overview of the CCP4 suite and current developments. *Acta Crystallogr. D Biol. Crystallogr.* 67:235–242. https://doi.org/10.1107/S0907444910045749

World Health Organization. 2019. International Travel and Health: Tick-borne Encephalitis. www.who.int/ith/diseases/tbe/en

Xu, M., R. Zuest, S. Velumani, F. Tukijan, Y.X. Toh, R. Appanna, E.Y. Tan, D. Cerny, P. MacAry, C.-I. Wang, and K. Fink. 2017. A potent neutralizing antibody with therapeutic potential against all four serotypes of dengue virus. *NPJ Vaccines.* 2:2. https://doi.org/10.1038/s41541-016-0003-3

Yang, X., J. Qi, R. Peng, L. Dai, E.A. Gould, G.F. Gao, and P. Tien. 2019. Molecular Basis of a Protective/Neutralizing Monoclonal Antibody Targeting Envelope Proteins of both Tick-Borne Encephalitis Virus and Louping Ill Virus. *J. Virol.* 93:e02132-18. https://doi.org/10.1128/JVI.02132-18

Ye, J., N. Ma, T.L. Madden, and J.M. Ostell. 2013. IgBLAST: an immunoglobulin variable domain sequence analysis tool. *Nucleic Acids Res.* 41(Web Server issue, W1):W34-W40. https://doi.org/10.1093/nar/gkt382

Yoshii, K. 2019. Epidemiology and pathological mechanisms of tick-borne encephalitis. *J. Vet. Med. Sci.* 81:343–347. https://doi.org/10.1292/jvms.18-0373

Zeman, P., and C. Bene. 2004. A tick-borne encephalitis ceiling in Central Europe has moved upwards during the last 30 years: possible impact of global warming? *Int. J. Med. Microbiol.* 293(Suppl 37):48–54. https://doi.org/10.1016/S1433-1128(04)80008-1

Zhao, H., L. Xu, R. Bombardi, R. Nargi, Z. Deng, J.M. Errico, C.A. Nelson, K.A. Dowd, T.C. Pierson, J.E. Crowe Jr., et al. 2020. Mechanism of differential Zika and dengue virus neutralization by a public antibody lineage targeting the DIII lateral ridge. *J. Exp. Med.* 217:e20191792. https://doi.org/10.1084/jem.20191792

Downloaded from http://rupress.org/jem/article-pdf/218/5/e20210236/1803798/jem_20210236.pdf by guest on 18 January 2024

JEM

Supplemental material

Downloaded from http://rupress.org/jem/article-pdf/218/5/e20210236/1803798/jem_20210236.pdf by guest on 18 January 2024

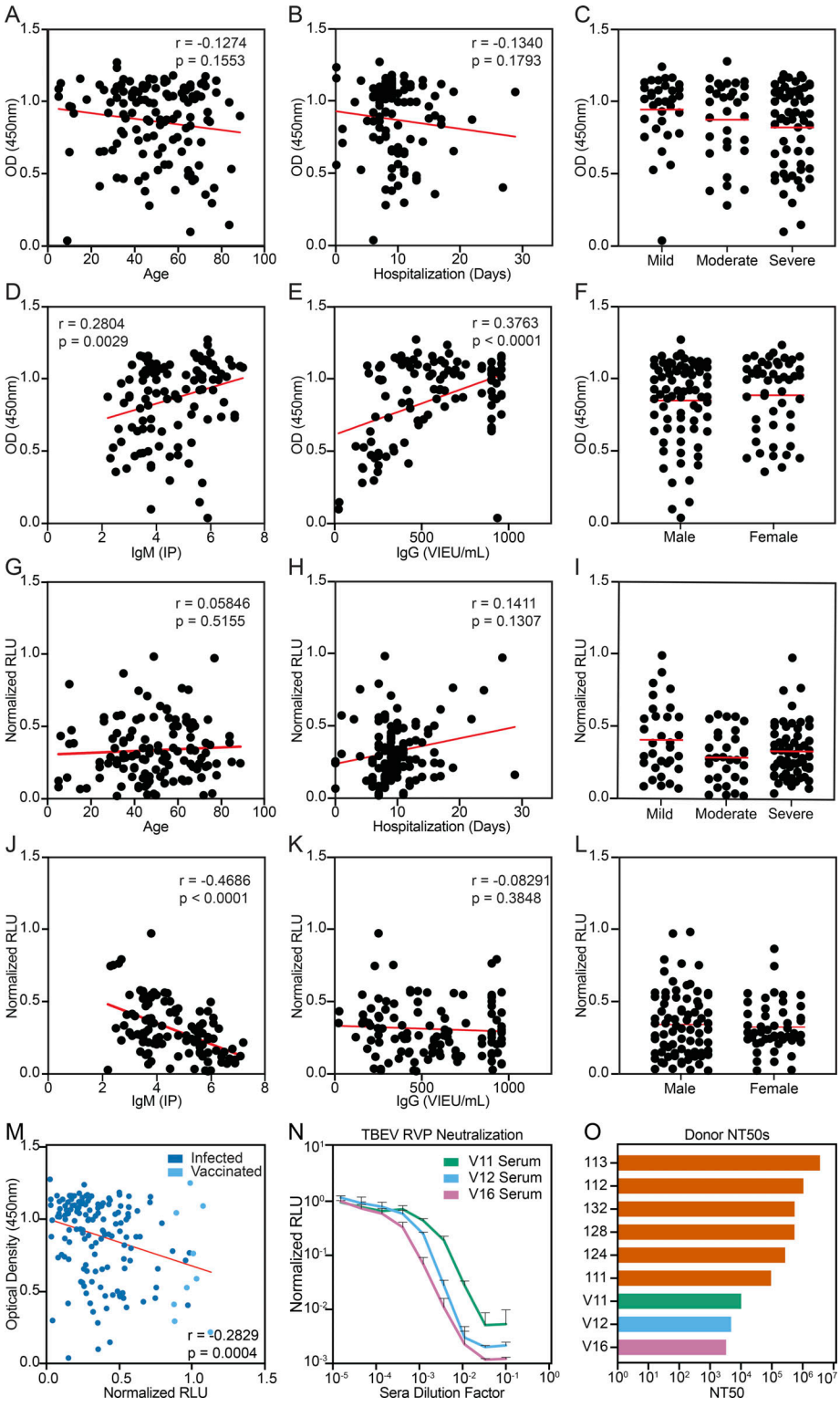

Figure S1. **Clinical correlations and serum neutralization in vaccinees. (A–F)** Serum TBEV EDIII ELISA data (IgG) from Fig. 1 B plotted against demographic and available clinical information. **(G–L)** Serum TBEV RVP neutralization data from Fig. 1 C plotted against demographic and available clinical information. A and G show age (no significance), B and H show length of hospitalization (no significance), C and I show severity of disease (no significant differences), D and J show IgM titers (IP) measured at the time of hospitalization ($P = 0.0029$ and $P < 0.0001$, respectively); E and K show IgG titers (Vienna units/ml) measured at the time of hospitalization ($P < 0.0001$ and no significance, respectively), and F and L show patient gender (no significant differences). Statistical significance was calculated for A, B, D, E, G, H, J, and K using two-tailed Spearman's tests; for L and F using Mann–Whitney tests; and for C and I using one-way ANOVA with Tukey's test. **(M)** Correlation between serum TBEV EDIII ELISA (IgG) and RVP neutralization data. **(N)** TBEV RVP neutralization curves with sera from vaccinated PBMC donors. Representative of two experiments, each performed in triplicate. Data are presented as mean with standard deviation. **(O)** Summary of serum NT_{50}s for all infected and vaccinated PBMC donors. Related to Fig. 1 and Table S1. RLU, relative light units.

Downloaded from http://rupress.org/jem/article-pdf/218/5/e20210236/1803798/jem_20210236.pdf by guest on 18 January 2024

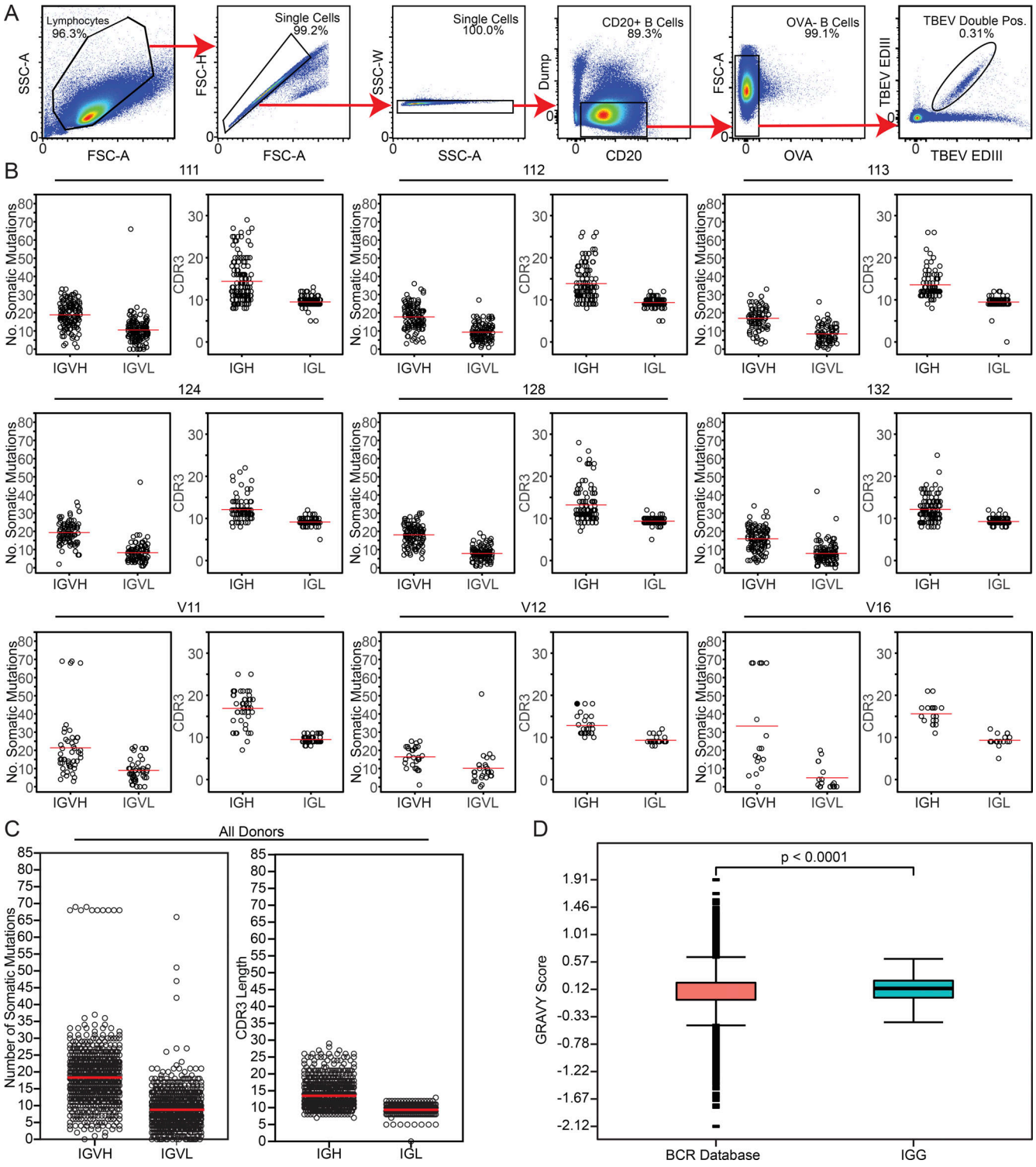

Figure S2. **Sorting strategy and antibody sequence analysis. (A)** Sorting strategy. Forward and side scatter (FSC and SSC, respectively) were used to gate on single lymphocytes. Dump channel included CD3, CD8, CD14, CD16, and a viability dye. CD20$^+$ B cells that failed to bind OVA (OVA$^-$) but did bind to the TBEV EDIII bait coupled with both PE and AF647 fluorophores were purified. **(B)** For each donor, the number of V gene somatic nucleotide mutations is shown on the left and the amino acid length of the CDR3 is shown on the right. **(C)** As in B, but for all donors combined. For B and C, horizontal red lines indicate the mean. **(D)** Distribution of hydrophobicity GRAVY scores at the IGH CDR3 of antibodies from all donors combined and compared with human repertoire (Briney et al., 2019). $P < 0.0001$ was determined using the Wilcoxon nonparametric test. Related to Fig. 2, Table S2, and Table S3.

Downloaded from http://rupress.org/jem/article-pdf/218/5/e20210236/1803798/jem_20210236.pdf by guest on 18 January 2024

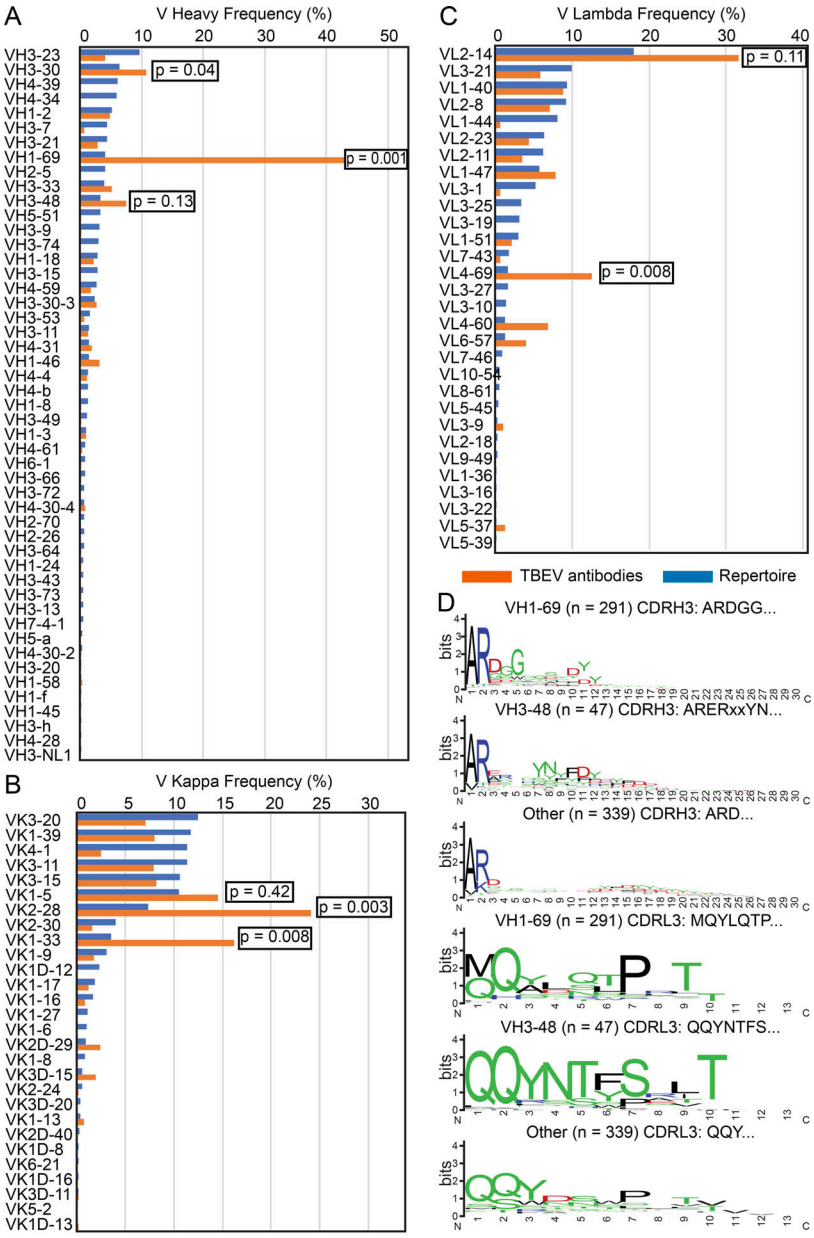

E

	HEAVY				LIGHT		
	IGHV	IGHD	IGHJ	CDRH3	IGLV	IGLJ	CDRL3
111	IGHV1-69*01	IGHD3-10*01	IGHJ4*02	ARDGGM--GSFDY	IGKV2-28*01	IGKJ2*01	MQALTPRT
132	IGHV1-69*01	IGHD3-10*01	IGHJ4*02	.....S--.....	IGVK2-28*01	IGKJ2*01	....
124	IGHV1-69*01	IGHD3-16*01	IGHJ4*02	..E..GIGP.L..	IGKV2-28*01	IGKJ2*01	....
113	IGHV1-69*01	IGHD1-26*01	IGHJ4*02	..E..AGA-.L..	IGVK2-28*01	IGKJ2*01	.....F..
112	IGHV1-69*01	IGHD3-10*01	IGHJ4*02	..V..L--..Y..	IGKV2-28*01	IGKJ2*01	......H.
128	IGHV1-69*01	IGHD3-10*01	IGHJ4*02	.....1--..L..	IGVK2-28*01	IGKJ2*01	..P...H.
112	IGHV1-69*01	IGHD5-18*01	IGHJ4*02	ATGYSY--GDY	IGKV1-33*01	IGKJ4*01	QHYNNLPLGT
124	IGHV1-69*01	IGHD5-18*01	IGHJ4*02	......--...	IGKV1-33*01	IGKJ4*01	....
128	IGHV1-69*01	IGHD5-18*01	IGHJ4*02	......--...	IGKV1-33*01	IGKJ4*01	...D...RL.
132	IGHV1-69*01	IGHD1-14*01	IGHJ4*02	.RA.GVTG...	IGKV1-33*01	IGKJ4*01	.Q..S..SL.
111	IGHV1-69*01	IGHD4-17*01	IGHJ4*02	.R.GA.GDYL.	IGKV1-33*01	IGKJ4*01	...DS..SV.
124	IGHV3-48*03	IGHD1-1*01	IGHJ4*02	ARPRNHYNLFDY	IGKV1-5*03	IGKJ4*01	QQNTYSALT
113	IGHV3-48*03	IGHD1-14*01	IGHJ4*02	..AG....Y..F	IGKV1-5*03	IGKJ4*01	....F..V.
111	IGHV3-48*03	IGHD3-10*01	IGHJ4*02	...FLGWGF..S	IGKV1-5*03	IGKJ4*01	....F.EI.

Figure S3. **Antibody V gene frequency and CDR3 sequences. (A)** Bar graph showing the frequency of V heavy gene usage in TBEV antibodies from infected donors compared with human repertoire (Rubelt et al., 2012). **(B and C)** As in A, but for V kappa and V lambda genes. In A–C, orange indicates anti-TBEV antibodies isolated in this study, while blue indicates control repertoire; P values were calculated using a two-tailed *t* test with unequal variances. **(D)** Sequence logos for antibody CDR3s from infected donors generated by WebLogo. The height of the stack indicates the sequence conservation at a given position, while the height of letters within the stack indicates the relative frequency of each amino acid at that position. **(E)** Examples of highly similar antibody sequences found in multiple donors. Related to Fig. 2, Table S2, and Table S3.

Downloaded from http://rupress.org/jem/article-pdf/218/5/e20210236/1803798/jem_20210236.pdf by guest on 18 January 2024

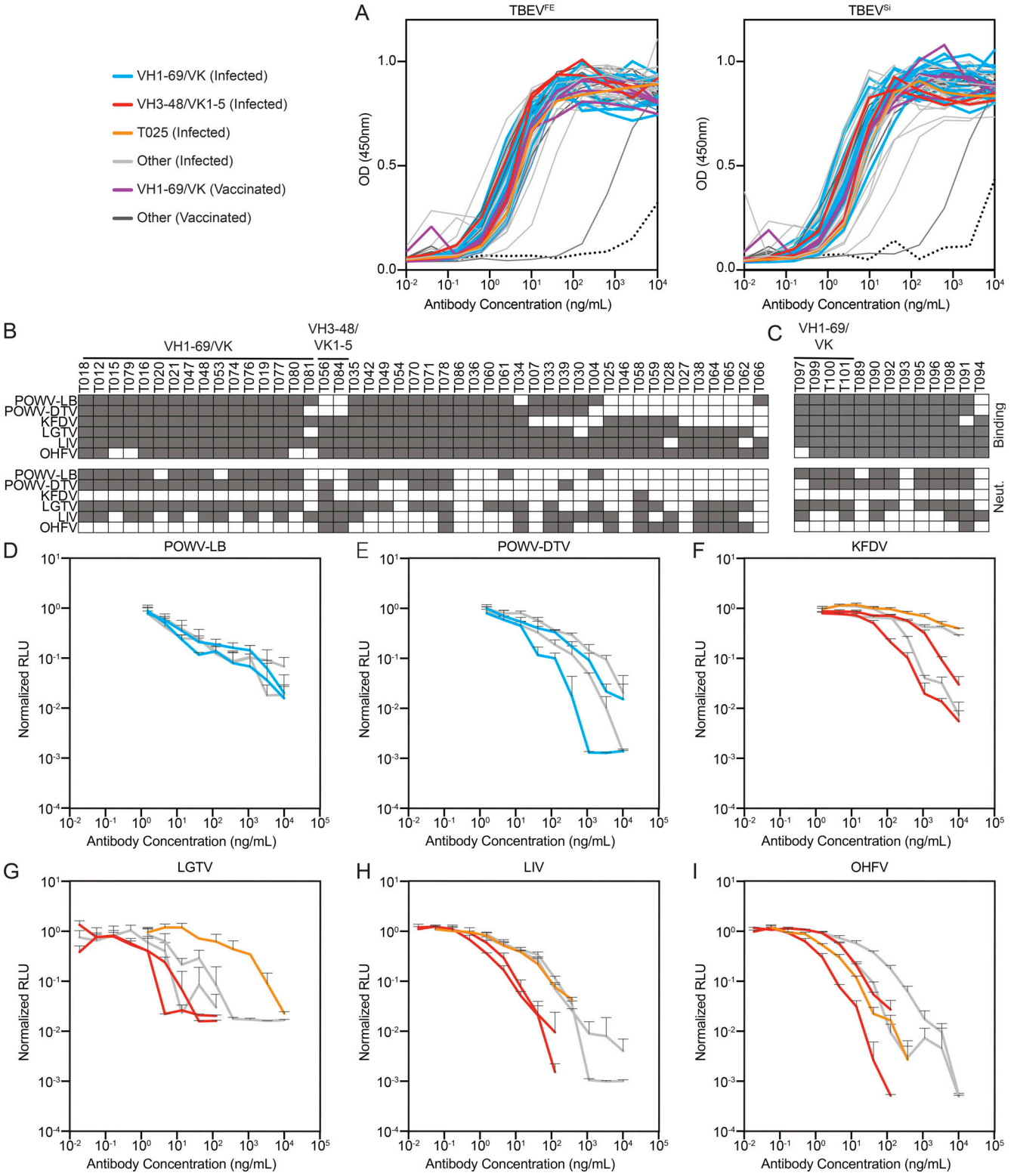

Figure S4. **Antibody binding and neutralization. (A)** ELISA binding curves to TBEV^{FE} and TBEV^{Si} EDIII for the 59 antibodies. Data are representative of two experiments. **(B)** Top panel shows screening for infected donor antibodies binding to a panel of tick-borne flavivirus EDIIIs, including POWV-LB, POWV-DTV, KFDV, LGTV, LIV, and OHFV. Antibodies were screened in duplicate at 1 µg/ml. Bottom panel shows screening for neutralization against RVPs corresponding to the same panel of tick-borne flaviviruses. Infected donor antibodies were screened in triplicate at 1 µg/ml. **(C)** Screening for vaccine antibodies binding and neutralization against a panel of tick-borne flavivirus EDIIIs and RVPs as in B. In B and C, gray indicates binding or neutralization over control. **(D–I)** Neutralization curves of selected antibodies against tick-borne flavivirus RVPs other than TBEV. Representative of two experiments in triplicate. Error bars indicate standard deviation. Related to Fig. 3, Table S4, and Table S5.

Downloaded from http://rupress.org/jem/article-pdf/218/5/e20210236/1803798/jem_20210236.pdf by guest on 18 January 2024

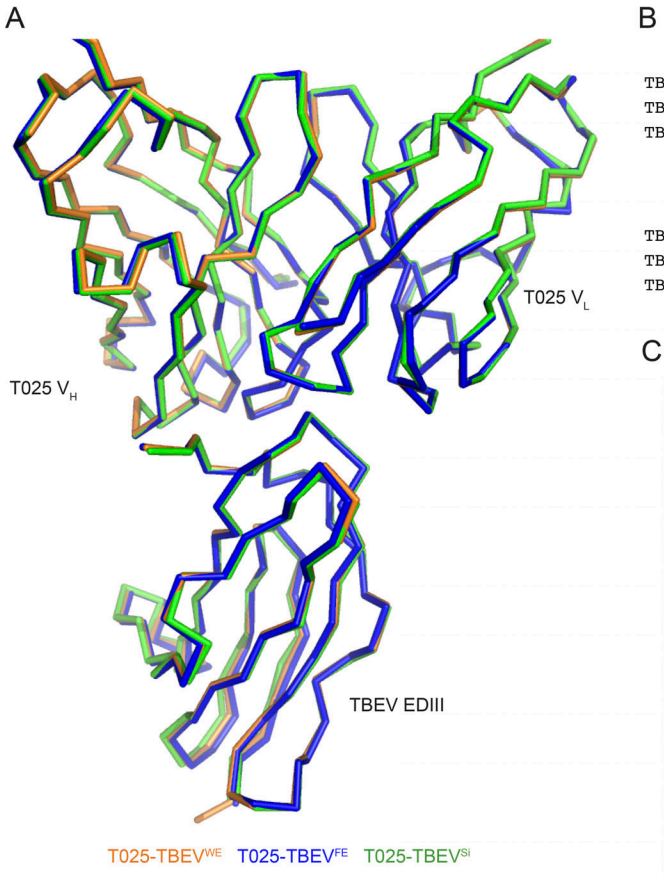

C

Antibody/Antigen Contacts

Chain	T025 Fab	TBEV-WE EDIII	Closest distance (Å)
HC	Y52A	K309	3.4
	I55	M306	3.9
	S56	T305, M306	2.9
	K57	T305	3.4
	S58	T305	4.0
	T97	D308, T310	2.7
	A98	D308, K309	3.0
	I99	T305, M306, D308	2.9
	D100	D308, K311, G334, T335	2.9
	P100A	K311, T335	3.7
LC	N32	S333, G334	3.1
	Y91	T335	2.7
	N92	G334, T335, K336	2.9
	N93	T335, K336, N366	2.9
	W94	T305, T335, K336, P337	2.9

Figure S5. **T025 antibody recognizes three subtypes of TBEV EDIII. (A)** Overlay of crystal structures of T025 Fab bound to EDIII from three subtypes of TBEV. Structures were aligned on all Cα atoms in the Fab–EDIII complex and shown as orange (T025-TBEV^{WE} EDIII), blue (T025-TBEV^{FE} EDIII), or green (T025-TBEV^{Si} EDIII) ribbons. RMSDs for Fab-EDIII alignments are 0.54 Å (T025-TBEV^{WE} EDIII and T025-TBEV^{FE} EDIII; 518 Cα atoms) and 0.26 Å (T025-TBEV^{WE} EDIII and T025-TBEV^{Si} EDIII; 525 Cα atoms). The C_HC_L domains of the Fabs were omitted for clarity. **(B)** Sequence alignment of EDIIIs from three strains of TBEV. Residues that contain an EDIII atom within 4 Å of an atom within a residue in T025 in each crystal structure are highlighted in orange. β-Strands are shown as arrows and defined according to Rey et al. (1995). **(C)** Contact residues between T025 Fab and TBEV^{WE} EDIII. Contacts were identified using AntibodyDatabase (West et al., 2013) and defined as residues in which any atom is within 4 Å of an atom from a residue on the interacting partner. Related to Fig. 4.

Tables S1–S6 are provided online as separate Excel and Word files. Table S1 lists clinical data from TBEV-infected and vaccinated donors. Table S2 lists sequences of anti-TBEV-EDIII IgG antibodies. Table S3 lists highly similar antibody sequences shared across individuals. Table S4 lists sequences of cloned recombinant monoclonal antibodies. Table S5 lists effective and inhibitory concentrations of recombinantly expressed monoclonal antibodies. Table S6 lists data collection and refinement statistics for the crystal structures.

Downloaded from http://rupress.org/jem/article-pdf/218/5/e20210236/1803798/jem_20210236.pdf by guest on 18 January 2024